ERDC/GSL TR-14-4

Geotechnical and Structures Laboratory

US Army Corps
of Engineers®
Engineer Research and
Development Center

ERDC
INNOVATIVE SOLUTIONS
for a safer, better world

An Investigation of Concrete Deterioration at South Florida Water Management District Structure S65E

Robert D. Moser, E. Rae Gore, Charles A. Weiss Jr.,
June E. Mirecki, Brian H. Green, and Robert V. Felice

February 2014

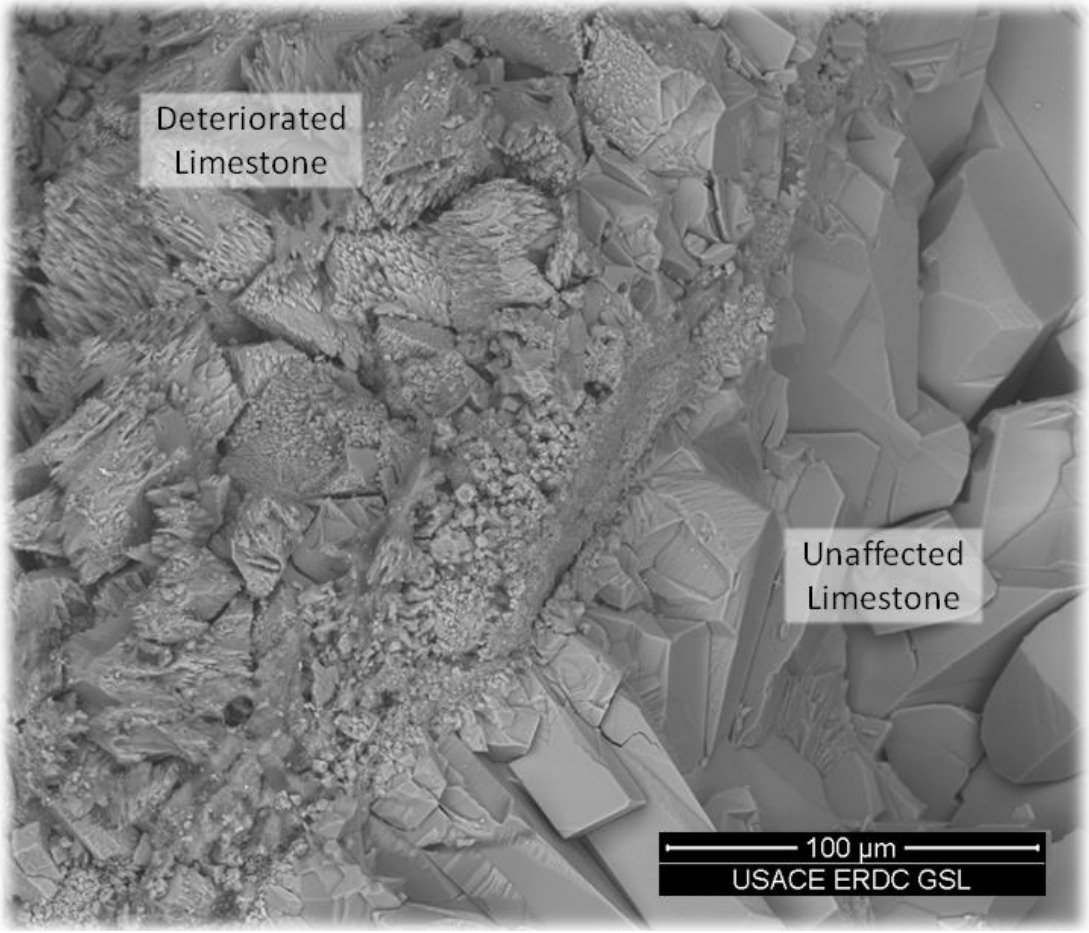

Approved for public release; distribution is unlimited.

The US Army Engineer Research and Development Center (ERDC) solves the nation's toughest engineering and environmental challenges. ERDC develops innovative solutions in civil and military engineering, geospatial sciences, water resources, and environmental sciences for the Army, the Department of Defense, civilian agencies, and our nation's public good. Find out more at www.erdc.usace.army.mil.

To search for other technical reports published by ERDC, visit the ERDC online library at http://acwc.sdp.sirsi.net/client/default.

ERDC/GSL TR-14-4
February 2014

An Investigation of Concrete Deterioration at South Florida Water Management District Structure S65E

Robert D. Moser, E. Rae Gore, Charles A. Weiss Jr.,
and Brian H. Green

Geotechnical and Structures Laboratory
US Army Engineer Research and Development Center
3909 Halls Ferry Road
Vicksburg, MS 39180-6199

June E. Mirecki

US Army Engineer District, Jacksonville
701 San Marco Blvd
Jacksonville, FL 32207

Robert V. Felice

US Army Engineer District, Tulsa
1645 S 101 E Ave
Tulsa, OK 74128

Final report

Approved for public release; distribution is unlimited.

Prepared for US Army Engineer District, Jacksonville
701 San Marco Blvd
Jacksonville, FL 32207

Under Rapid Assessment of Concrete Deterioration at S65E

Abstract

This report documents the findings of a concrete deterioration study of South Florida Water Management District Structure S65E. The study examined water quality at the S65E site and concrete cores from deteriorated, repaired, and non-deteriorated areas of the structure. In addition, a geochemical water-rock reaction simulation was performed to investigate the potential for dissolution of the concrete based on local water quality. The predominant form of deterioration observed was severe loss of both paste and coarse aggregates from the surface of the concrete with larger losses in high-flow areas of dam piers than in the lock chamber. Concrete from deteriorated areas exhibited significant loss of Pleistocene limestone coarse aggregates and paste, while the siliceous, fine aggregates were unaffected. Concrete distress may be caused by dissolution of soluble phases and biodeterioration, which can result in localized acidification at the surface and direct or chemical consumption of mineral phases present in concrete. The use of siliceous aggregates, along with efforts to minimize porosity/permeability, and improved acid resistance would likely improve the durability of the repair material, as well as better protect the underlying concrete from subsequent deterioration.

DISCLAIMER: The contents of this report are not to be used for advertising, publication, or promotional purposes. Citation of trade names does not constitute an official endorsement or approval of the use of such commercial products. All product names and trademarks cited are the property of their respective owners. The findings of this report are not to be construed as an official Department of the Army position unless so designated by other authorized documents.

DESTROY THIS REPORT WHEN NO LONGER NEEDED. DO NOT RETURN IT TO THE ORIGINATOR.

Contents

Figures and Tables

Figures

Tables

Executive Summary

This report documents the findings of a concrete deterioration study of South Florida Water Management District Structure S65E. US Army Engineer Research and Development Center (ERDC) personnel in the Concrete and Materials Branch of the Geotechnical and Structures Laboratory provided technical assistance in the forensic examination of the concrete. The study examined water quality at the S65E site and concrete cores from deteriorated, repaired, and non-deteriorated areas of the structure. In addition, a geochemical water-rock reaction simulation was performed to investigate the potential for dissolution of the concrete based on local water quality. The predominant form of deterioration observed was severe loss of both paste and coarse aggregates from the surface of the concrete with larger losses in high-flow areas of dam piers than in the lock chamber. Water quality measurements found negligible concentrations of SO_4^{2-} and Cl^-. Historical water quality records indicated that the carbonate alkalinity was generally low at S65E, suggesting the potential in the concrete for active dissolution of soluble components, such as portlandite ($Ca(OH)_2$) and the limestone ($CaCO_3$-based) aggregates. The pH was measured and found to be neutral at approximately 7. X-ray diffraction analysis of various components and regions in the concrete showed evidence of minor carbonation and leaching of soluble phases from the surface of the concrete but no evidence of deterioration resulting from sulfate attack. Petrographic analysis of concrete from non-deteriorated areas showed minor carbonation but no other detectable deterioration. Concrete from deteriorated areas exhibited significant loss of Pleistocene limestone coarse aggregates and paste, while the siliceous, fine aggregates were unaffected. The shotcrete repair material appeared to have a good bond with the concrete substrate but was extremely porous and also contained limestone aggregates, which were found to be prone to deterioration in the original concrete at S65E. High-magnification photomicrographs obtained using scanning electron microscopy confirmed dissolution of the limestone coarse aggregates at the surface, while siliceous fine aggregates were unaffected. These results suggest that sulfate attack, acid attack, Cl- induced corrosion, or other typical forms of concrete deterioration are likely not the cause(s) of the observed deterioration. Concrete distress may be caused by dissolution of soluble phases and biodeterioration, which can result in localized acidification at the surface and direct or chemical consumption of mineral phases

present in concrete (e.g., CaCO3). The use of siliceous aggregates, along with efforts to minimize porosity/permeability (e.g., low w/cm, use of water reducing admixtures), and improved acid resistance (e.g., use of silica fume) would likely improve the durability of the repair material, as well as better protect the underlying concrete from subsequent deterioration.

Preface

This study was conducted in support of the US Army Engineer District, Jacksonville, as a rapid assessment of concrete deterioration at South Florida Water Management District Structure S65E. The technical monitor was Dr. Charles A. Weiss, Jr., of the US Army Engineer Research and Development Center (ERDC).

The research was performed by personnel of the Concrete and Materials Branch (CMB), Engineering Systems and Materials Division (ESMD), Geotechnical and Structures Laboratory (GSL), ERDC. Dr. Robert D. Moser led the study and performed the microscopy work. E. Rae Gore performed the X-ray diffraction analysis. Dr. Weiss provided oversight on the experimental work. Brian H. Green provided input on the proposed repair options and deterioration mechanisms. Robert V. Felice of the US Army Engineer District, Tulsa, assisted with the laboratory work and sample preparation. Dr. June E. Mirecki of the Jacksonville District performed geochemical water-rock interaction models to investigate concrete dissolution in South Florida waters.

At the time of publication, Christopher M. Moore was Chief, CMB; Dr. Larry N. Lynch was Chief, ESMD; Dr. William P. Grogan was Deputy Director, GSL; and Dr. David W. Pittman was Director, GSL. Dr. David A. Horner was the lead Technical Director within GSL.

COL Jeffrey R. Eckstein was Commander and Executive Director of ERDC. Dr. Jeffery P. Holland was Director.

1 Scope

The Concrete and Materials Branch (CMB), Geotechnical and Structures Laboratory (GSL), US Army Engineer Research and Development Center (ERDC) was requested to perform an analysis of concrete deterioration occurring at inland navigation structure S65E, owned and operated by the South Florida Water Management District (SFWMD). The request for ERDC assistance was made in conjunction with work being conducted by the US Army Engineer District, Jacksonville, in collaboration with the SFWMD. An aerial view of structure S65E is provided in Figure 1.

Figure 1. Aerial view of lock and dam structure S65E.

Concrete deterioration reported to ERDC by the Jacksonville District personnel focused on significant deterioration of the surface of the concrete. A photograph of typical concrete deterioration observed in an area where concrete cores were extracted is shown in Figure 2.

Figure 2. Typical concrete deterioration at location where concrete core was extracted.

In coordination with Jacksonville District personnel, concrete core samples were extracted and shipped to ERDC along with water samples collected at the site. Concrete was cored from non-deteriorated, deteriorated, and repaired areas of the structure. Seven cores were received: three from deteriorated areas, two from repaired areas, and two from non-deteriorated areas. A summary of cores received is provided in Table 1. Four of the seven cores received were used for analysis. Figure 3 shows an image of surface deterioration observed in as-received cores from deteriorated areas of S65E.

Table 1. Summary of concrete cores obtained from S65E.

CMB Serial No.	Attribute/Notes	Analyzed (Yes/No)
130036_D1	Concrete core from deteriorated area in dam pier	No
130036_D2	Concrete core from deteriorated area in dam pier	Yes
130036_D3	Concrete core from deteriorated area in lock chamber	Yes
130036_R1	Concrete core including shotcrete repair	Yes
130036_R2	Concrete core including shotcrete repair	No
130036_N1	Concrete core from non-deteriorated area	Yes
130036_N2	Concrete core from non-deteriorated area	No

Figure 3. As-received concrete cores from deteriorated areas of S65E.

A geochemical model was developed to simulate water-rock interactions at two locations: S65A, where concrete deterioration is present, and S5A (south of Lake Okeechobee), where concrete deterioration is absent. Historical water quality data obtained from the SFWMD database DBHydro supplement analyses obtained for this study. The geochemical model simulations tested the hypothesis that surface water quality at S65A facilitated concrete deterioration by dissolution of certain concrete components, specifically limestone (calcium carbonate, $CaCO_3$) aggregate and portlandite in the paste.

Forensic examinations of the as-received concrete cores consisted of visual examination of the cores, petrographic analysis using stereomicroscopy, X-ray diffraction to examine changes in mineralogy in various regions of the concrete, high-resolution imaging, and chemical analysis using scanning electron microscopy (SEM) and energy-dispersive X-ray spectroscopy.

The following chapters provide details on the analysis methods employed, the results obtained, and the conclusions and recommendations of the study.

2 Testing Methods

Testing focused on water quality measurements and various techniques to forensically examine concrete cores from deteriorated, repaired, and non-deteriorated areas of S65E. The following sections describe the methods used.

2.1 Extraction of concrete cores

Coring of concrete from ECMs was performed by personnel coordinated by the Jacksonville District according to the provisions outlined in ASTM C42 - *Standard test method for obtaining and testing drilled cores and sawed beams of concrete*.

2.2 Water quality measurements

Samples of water from the S65E site were collected by on-site personnel and shipped back to ERDC for analysis. Two approximately 50-ml vials were filled with water. One vial was used for pH, SO_4^{2-}, and Cl^- analysis. The second vial, which included approximately 2 ml of HNO_3 to acidify the water, was used for metal analysis including Al, Fe, Mg, P, K, Na, Ca, Cu, Pb, Mn, Mo, Ni, Se, Ag, Sb, Th, V, Zn, As, Ba, Be, Cd, Cr, and Co. Chemical analyses were performed by the Environmental Chemistry Branch, Environmental Laboratory, ERDC, using inductively coupled plasma mass spectroscopy (ICP-MS). The pH measurements were performed by personnel in the ERDC CMB.

2.3 Geochemical water-rock reactions

In order to assess the potential for dissolution of various components present in the concrete, a geochemical water-rock reaction simulation was performed using historical water quality data. Geochemical reactions between concrete components and representative surface water compositions were compared at two locations: (1) north of Lake Okeechobee, using surface water quality data from the Kissimmee River aquifer storage recovery (KRASR) pilot system near S65E, and (2) south of Lake Okeechobee, using surface water quality data from structure S-5A, located on C-51 at the northern end of water conservation area (WCA) 1. The concrete components analyzed included calcite and dolomite (to represent

coarse limestone aggregate), portlandite ($Ca(OH)_2$) in the paste, and quartz (to represent fine silica aggregate in the paste).

Water-rock interaction models were run using PHREEQC v. 2.17 (Parkhurst and Appelo 1999 and subsequent updates) to evaluate how surface water interacts geochemically with concrete components under equilibrium thermodynamic conditions. Mineral saturation indices were calculated to determine whether calcite and dolomite (mineral components of limestone rock), portlandite, and quartz would dissolve or remain as a stable solid in contact with each surface water sample. Positive saturation indices indicate a stable solid; negative saturation indices indicate that the mineral will dissolve.

2.4 Petrographic analysis

Potential modes of distress--including sulfate attack, acid attack, micro-cracking, and overall concrete quality--were assessed by petrographic analysis performed on polished cross sections in accordance with ASTM C856 - *Standard practice for petrographic examination of hardened concrete*. Four concrete cores were examined: two from deteriorated areas (one from the lock chamber and one from the dam), one from a repaired area, and one from a non-deteriorated area. Cross sections of the 4-in. cores were cut and prepared for the petrographic analysis. The sections for petrographic analysis were polished using alumina suspensions in water to a particle size of 5 μm. Polished samples were imaged using a Zeiss Stereo Discovery V12 microscope at magnifications of 5 X to 40 X. An overall image was obtained of each sample at low magnification, and at least three selected sites were also imaged at higher magnification. Specific focus was given to microcracking, air void structure, aggregate deterioration, surface discoloration, surface dissolution/loss of material, and any other possible modes of concrete deterioration. A phenolphthalein pH indicator was also used to determine the depth of carbonation/acidification of the concrete in samples from deteriorated and non-deteriorated concrete in S65E. This indicator exhibits a bright pink color when exposed to alkaline concrete and remains clear when concrete is carbonated (pH below ~10).

2.5 X-ray diffraction analysis

X-ray diffraction (XRD) analysis was performed on samples extracted from a variety of regions of concrete. Samples of the coarse and fine aggregates and hydrated cement paste were extracted from non-

deteriorated areas of concrete. A bulk sample (i.e., mixture of paste and coarse and fine aggregates) was also prepared. Finally, samples were chipped from deteriorated areas of the surface concrete for analysis. The primary goal of these studies was to provide comparisons between the mineralogy present in the surface of deteriorated concrete and the bulk non-deteriorated concrete.

Once the desired sample was isolated from the concrete, it was crushed and ground until at least 90 percent of the material passed a #325 sieve (44 μm). Ground specimens were prepared into random powder pack sample holders for XRD measurements. Diffraction patterns to be used for qualitative phase identification were obtained using a Panalytical X'Pert Pro materials research diffractometer equipped with a Co-Kα X-ray source operated at 45 kV and 40 mA. Diffraction patterns were obtained over a period of 2 hr from 2° to 70° 2Θ with a step size of 0.002°. Phase identification was performed using MDI Jade2010 powder diffraction file (PDF) reference databases.

2.6 Scanning electron microscopy

Two specimens were examined using SEM to obtain high-resolution images. One specimen extracted directly from the exposed surface of the concrete was examined to observe deterioration and identify any biological growth present on the surface. The second specimen consisted of a 1-in.-diameter microcore extracted from the surface of the concrete and split longitudinally to expose a fractured surface, which extended from the exposed deteriorated surface to the inner non-deteriorated concrete. SEM imaging was performed using an FEI Nova NanoSEM 630 that is capable of high-resolution imaging on non-conductive materials. Imaging was performed in low-vacuum mode at pressures of 0.1 mbar and accelerating voltage of 15 kV. All images were acquired using a backscattered electron detector to improve phase contrast. Imaging was performed at three random sites and at various levels of magnification to capture the overall microstructure along with specific regions of interest (e.g., aggregate interfaces, cracks, and air voids).

3 Results and Discussion

3.1 Water quality and geochemical reactions

3.1.1 Water quality measurements

The results of water quality measurements are provided in Table 2. No measureable concentrations of Al, Pb, Mo, Se, Ag, Sn, Th, Ar, Be, Cd, Cr, or Co were found. No concentrations of any substance observed in solution would cause concern for potential concrete deterioration, including extremely low sulfate and chloride concentrations of 15.1 and 27.8, respectively. The measured pH of the water at S65E was 7.2, which causes no concern related to acid attack of typical structural concretes like that at S65E. These results suggest that the local water at S65E provides no major source of ions/pH that would lead to concentration. However, these results and conclusions are based only on analysis of grab samples that represent a snapshot in time. Long-term monitoring results could vary greatly depending on rainfall, season, and the presence of any industrial and/or agricultural activities upstream that may introduce effluents that could have an impact on water quality, which in turn could impact concrete durability.

Table 2. Results of water quality measurements.

Element/Compound	Concentration (mg/L) or (ppm)
Chloride (Cl-)	27.8
Sulfate (SO42-)	15.1
Iron (Fe)	0.214
Magnesium (Mg)	4.62
Phosphorus (P)	0.0508
Potassium (K)	2.98
Sodium (Na)	14.6
Calcium (Ca)	19.1
Copper (Cu)	0.0011
Manganese (Mn)	0.0057
Nickel (Ni)	0.0012
Vanadium (V)	0.0011
Zinc (Zn)	0.0189
Barium (Ba)	0.0135

3.1.2 Geochemical water-rock reactions

Median values of dissolved inorganic constituent concentrations in surface water samples at each location are shown in Table 3. Median values were calculated from large data sets (n=62 at S-5A and n=35 at the Kissimmee River ASR system (KRASR)) that were obtained from 2010 through 2013 during wet and dry seasons. KRASR is located approximately 5 miles downstream of S-65E and supplements analyses obtained there. Low percent charge balance errors (< 6 percent) indicate that these representative analyses are internally consistent.

Table 3. Median concentrations of major dissolved inorganic constituents measured in surface waters at S-5A (south of Lake O.) and at Kissimmee River ASR (north of Lake O., downstream from S-65E). Period of record: January 2010 to March 2013 for both sites. S-5A water quality data from SFWMD DBHydro. Kissimmee River water quality data from the Kissimmee River ASR pilot project.

	Dissolved Inorganic Constituents Concentrations in (mg/L) or (ppm)										
Location	Ca	Mg	Na	K	Cl	S	Si	Fe	pH	Total Carbonate Alkalinity	Charge Balance Error, in %
C-51 at S-5A	83	16.5	76	7.7	110	53	10	0.18	7.8	151	5.3
Kissimmee River at KRASR	19	6.9	16	4	31	16	1.2	0.26	6.7	48	3.4

There are obvious differences in surface water quality between these two sites. The concentrations of all dissolved inorganic constituents are much lower in the Kissimmee River compared to C-51 at S-5A. Carbonate alkalinity values in the lower Kissimmee River are one-third that at S5a. This strongly suggests that surface water is undersaturated with respect to CaCO3, resulting in dissolution of the solid phase. Also, pH values are neutral in the Kissimmee River and slightly alkaline in C-51 at S-5A. Water quality differences are consistent with the surface geology at the respective sites. The Kissimmee River Basin is characterized by siliceous sediments, whereas the L-8 Basin consists of carbonates and carbonate-cemented silicate sands.

Results of PHREEQC geochemical water-rock reaction calculations are shown in Table 4. At the S-5A water control structure, saturation indices are positive for all mineral components, indicating that calcite, dolomite, and quartz exist as stable solids and will not dissolve in contact with C-51 surface water. This is consistent with the observation that concrete deterioration is not observed at structures located south of Lake Okeechobee.

Table 4. Saturation indices (SI) for common minerals in aggregate. Positive SI values indicate that the mineral is a stable solid in contact with the water solution; negative SI values indicate that the mineral will dissolve in contact with the water solution.

Location	Mineral Saturation Index			
	Calcite	Dolomite	Quartz	Portlandite
	CaCO3	Ca,Mg (CO3)2	SiO2	Ca(OH)2
C-51 at S-5A	0.36	0.49	0.2	-10.21
Kissimmee River	-1.6	-3.4	-0.72	-12.84

At the Kissimmee River location, saturation indices are negative for all mineral components, indicating that calcite, dolomite, portlandite, and even quartz will dissolve in contact with Kissimmee River water. This is consistent with the observed concrete deterioration at S65E. Limestone ($CaCO_3$) aggregate deterioration can occur by inorganic dissolution reactions, will proceed in the absence of biofilms, and occur at neutral pH. Inorganic dissolution from contact with Kissimmee River surface water can explain the regional occurrence of concrete degradation in the Kissimmee River Basin. The negative saturation index value for quartz (-0.72) in contact with Kissimmee River surface water also indicates dissolution. Quartz dissolution is a rate-controlled reaction, unlike calcite and dolomite dissolution. Low silica concentrations in Kissimmee River water (1.2 mg/L, Table 3) indicate that quartz dissolution is possible, but other factors will control the rate of quartz dissolution at the ambient pH (7.8). Consequently, quartz dissolution is not observed in the S-65 concrete structures. The negative saturation index values for portlandite at both locations indicate dissolution of this paste component in contact with Kissimmee River and C-51 surface water, as is typical given the high aqueous solubility (2.5 g/L) of this mineral.

3.2 Petrographic analysis

3.2.1 Assessment of bulk concrete

Prior to examination of non-deteriorated, repaired, and deteriorated concrete from near the exposed surface, an examination of the bulk concrete was made to assess concrete quality and identify coarse and fine aggregates. Typical photomicrographs of the bulk concrete are shown in Figure 4. The concrete appeared to be competent and of high quality. Coarse aggregates were primarily a Pleistocene limestone commonly used in concrete in Florida. Fine aggregates were primarily siliceous. No evidence of deterioration was observed in the bulk concrete that was isolated from any surface deterioration present in the as-received concrete cores.

Figure 4. Photomicrographs of typical bulk concrete showing distribution in air voids, coarse aggregates, fine aggregates, and paste.

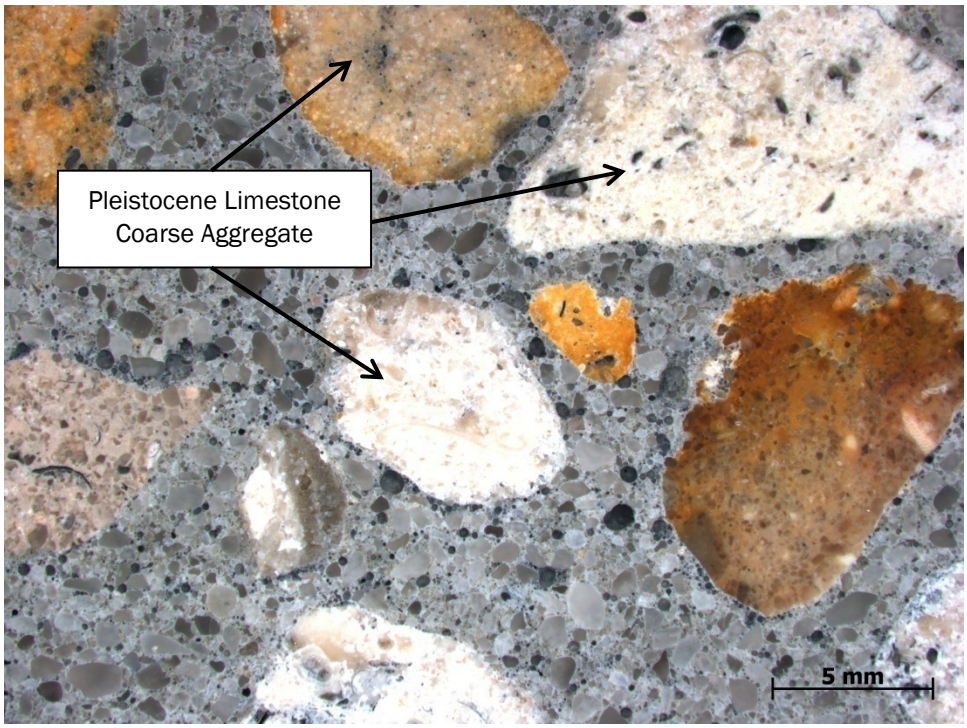

a. Low magnification photomicrograph.

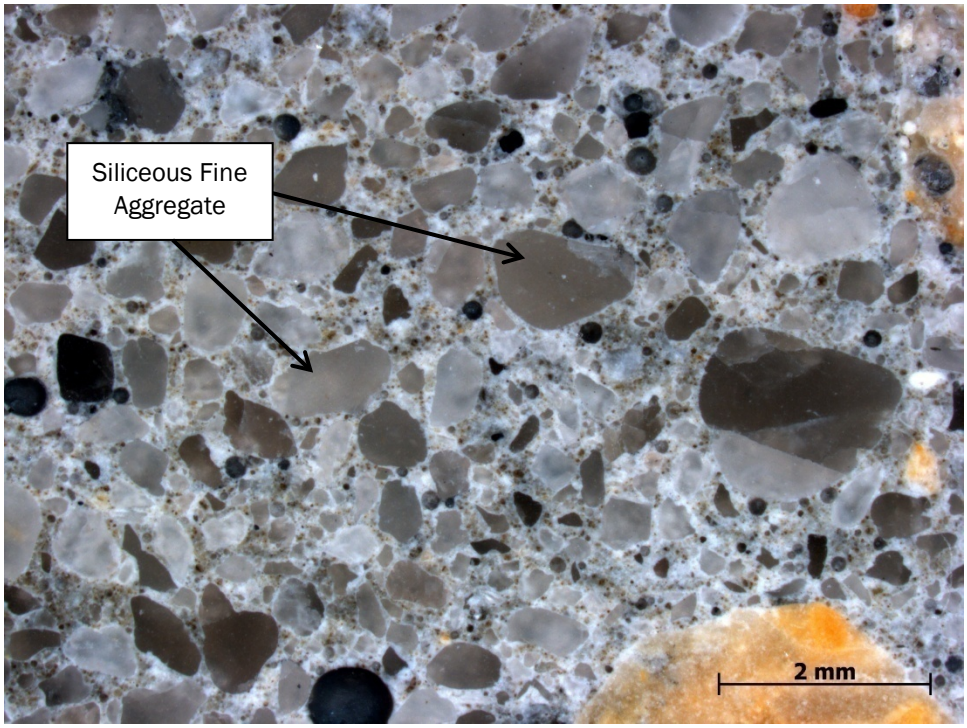

b. High magnification photomicrograph.

3.2.2 Non-deteriorated concrete surface

The condition of non-deteriorated concrete surfaces of as-received core 130036_N1 was examined using stereomicroscopy. Figure 5 shows typical photomicrographs obtained from cross sections of the non-deteriorated surface concrete. Similar to the bulk concrete, the coarse aggregate was a Pleistocene limestone, and the fine aggregate was siliceous. The non-deteriorated surface was extremely planar and well finished. A surface paint/coating layer was also evident in the as-received cores. A layer of discoloration was observed to penetrate to a depth of approximately 1.5 to 2 mm from the surface. The discoloration is likely associated with carbonation of the surface concrete by slow reaction of $Ca(OH)_2$ present in the concrete with atmospheric CO_2. The presence of carbonation was confirmed with the use of the phenolphthalein pH indicator solution (see Figure 6). Other than the minimal carbonation observed, no other evidence of distress was observed in concrete from non-deteriorated areas of the structure.

3.2.3 Repaired concrete surface

Concrete that was previously repaired due to deterioration of the original concrete at S65E was also examined. Figure 7 shows the typical microstructure observed in the shotcrete repair material. The shotcrete material contained a mixture of limestone and siliceous aggregates. The shotcrete was also found to be highly porous. The surface of the as-received repaired concrete had higher surface roughness than the original concrete examined from non-deteriorated areas of the structure (see Figure 8 of shotcrete surface vs. Figure 5 of original concrete surface). It is unclear whether this surface roughness is related to subsequent deterioration following application of the repair shotcrete or whether the initial finish of the shotcrete repair exhibited increased roughness.

The interface between the shotcrete repair material and the original concrete substrate, which had damaged concrete removed by hydroblasting, was also examined. Figure 9 shows examples of the typical interface observed between original concrete and the shotcrete repair material. Overall, the interface between the shotcrete and the original concrete substrate appeared to be well bonded. However, sparse porosity and delaminations were observed at the interface, which corroborates the findings presented in a report provided to ERDC by Jacksonville District personnel.

Figure 5. Photomicrographs of typical concrete at surface of non-deteriorated areas of S65E.

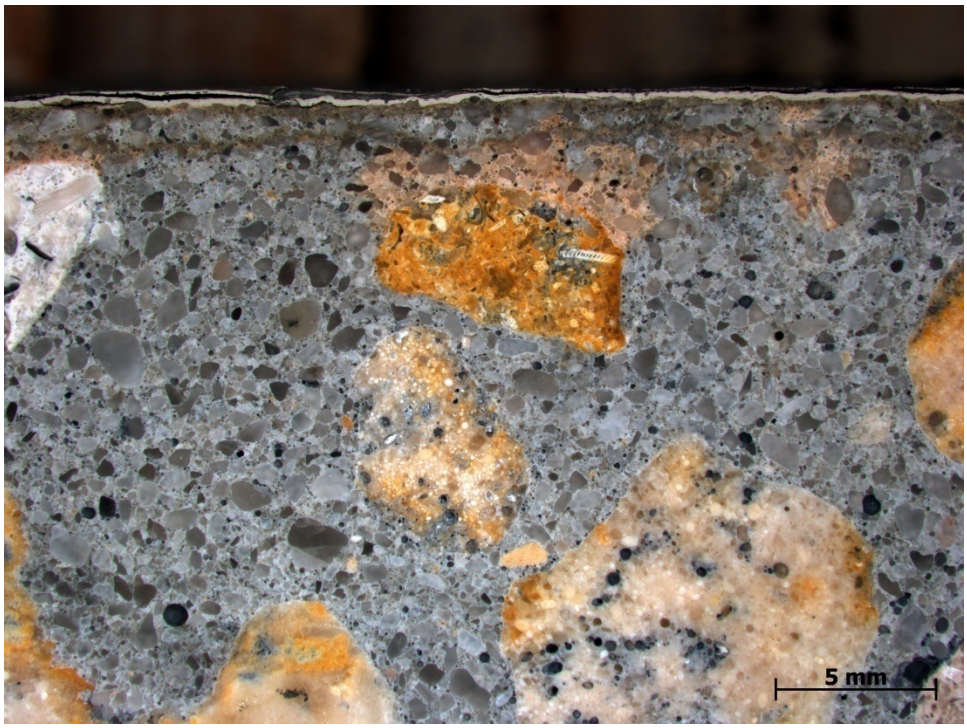

a. Low magnification photomicrograph.

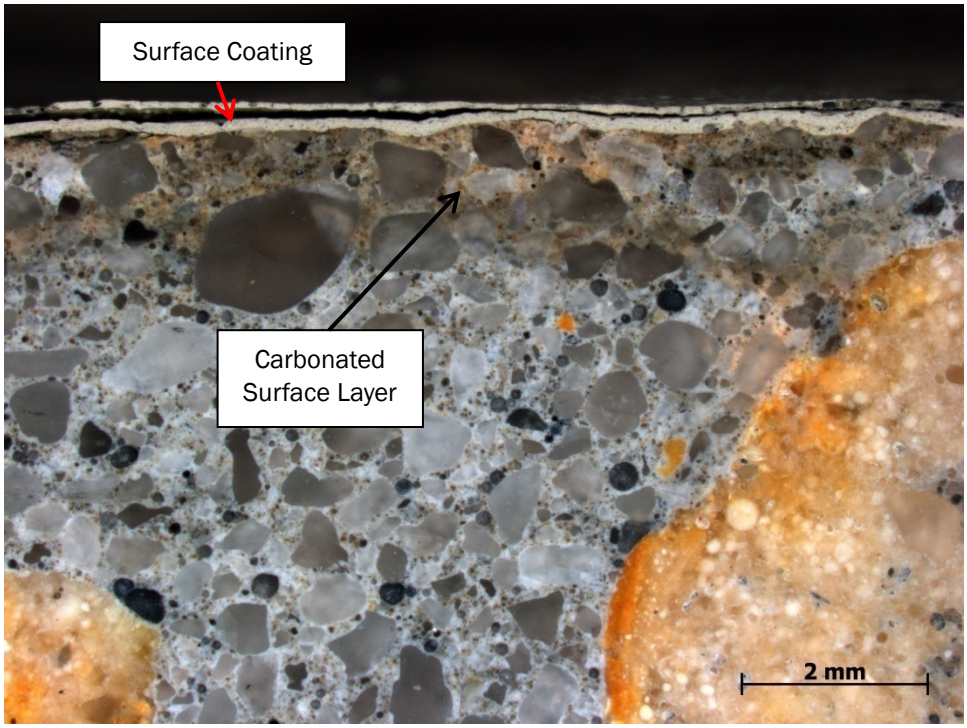

b. High magnification photomicrograph.

Figure 6. Surface of non-deteriorated concrete showing depth of carbonation using phenolphthalein pH indicator solution.

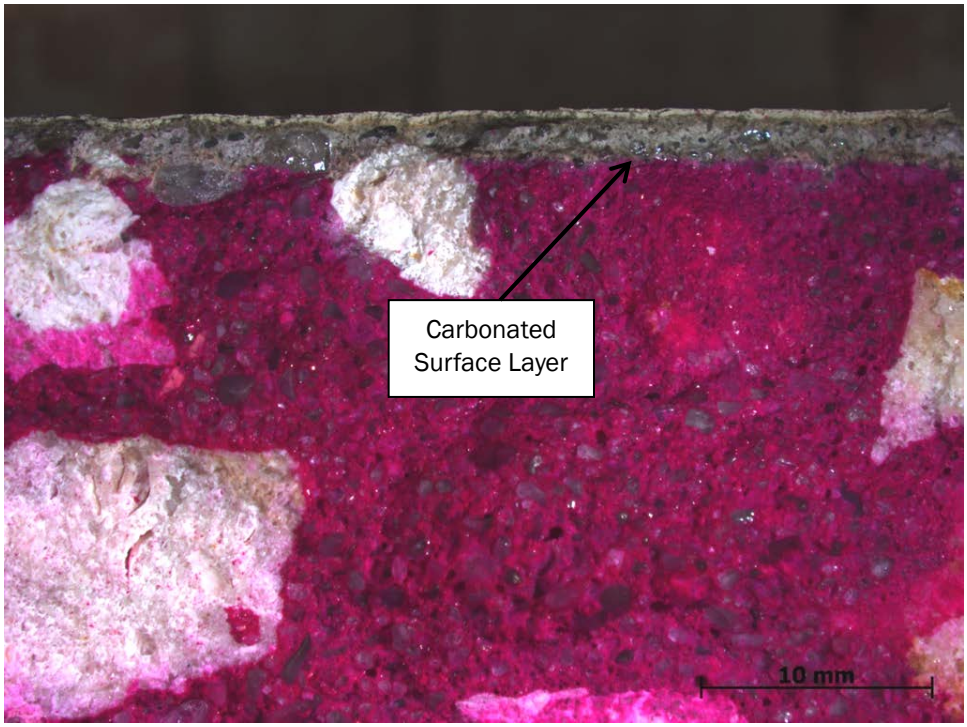

Figure 7. Typical microstructure of shotcrete used for repair, which consisted of limestone and siliceous aggregates and significant porosity.

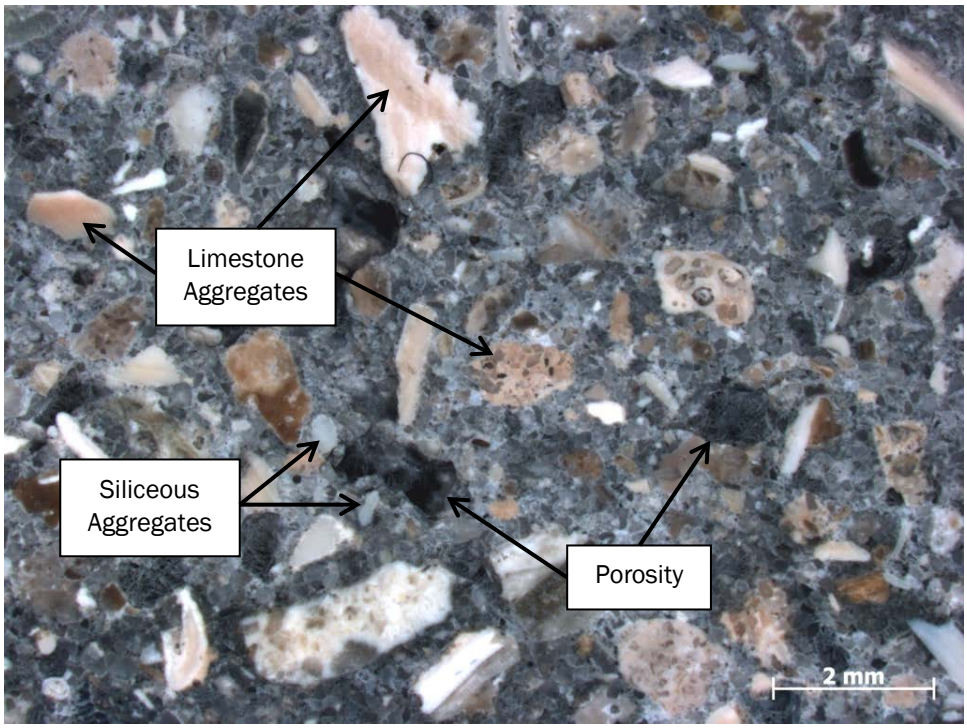

Figure 8. Photomicrograph of surface of shotcrete repair material showing high roughness.

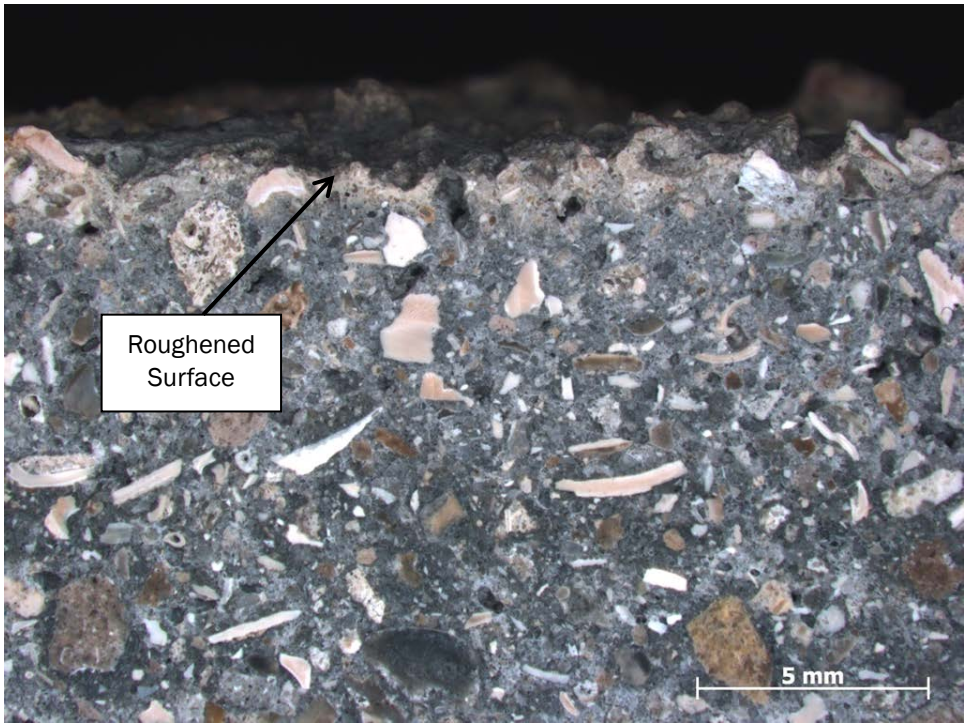

3.2.4 Deteriorated concrete surface

The primary focus of the petrographic analyses conducted was to investigate distress on cores from deteriorated areas of the structure. Concrete was examined from two deteriorated locations in the structure: (1) concrete from high flow rate areas in dam piers and (2) concrete from low flow rate areas in the lock chamber. Figures 10 and 11 show typical surface distress observed in deteriorated concrete from the dam and lock chamber, respectively.

Deterioration in concrete from the dam had reached depths approaching 25 mm, which was approximately half of the cover depth observed over embedded reinforcing steel. Concrete from the lock chamber only exhibited deterioration to a depth of approximately 10 mm. It is hypothesized that the increased depth of deterioration in concrete from the dam may be related to the increased flow rates in the spillway when compared with flow velocities to which concrete surfaces in the lock chamber are exposed.

Figure 9. Photomicrographs of typical interface between the shotcrete repair material and the original concrete substrate.

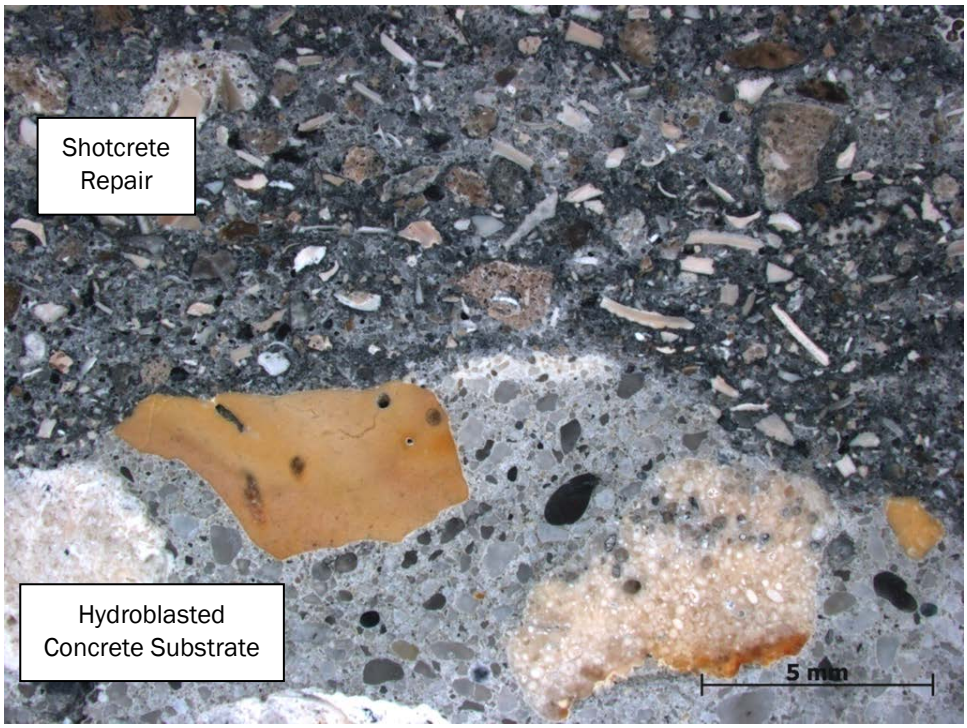

a. Typical repair interface #1.

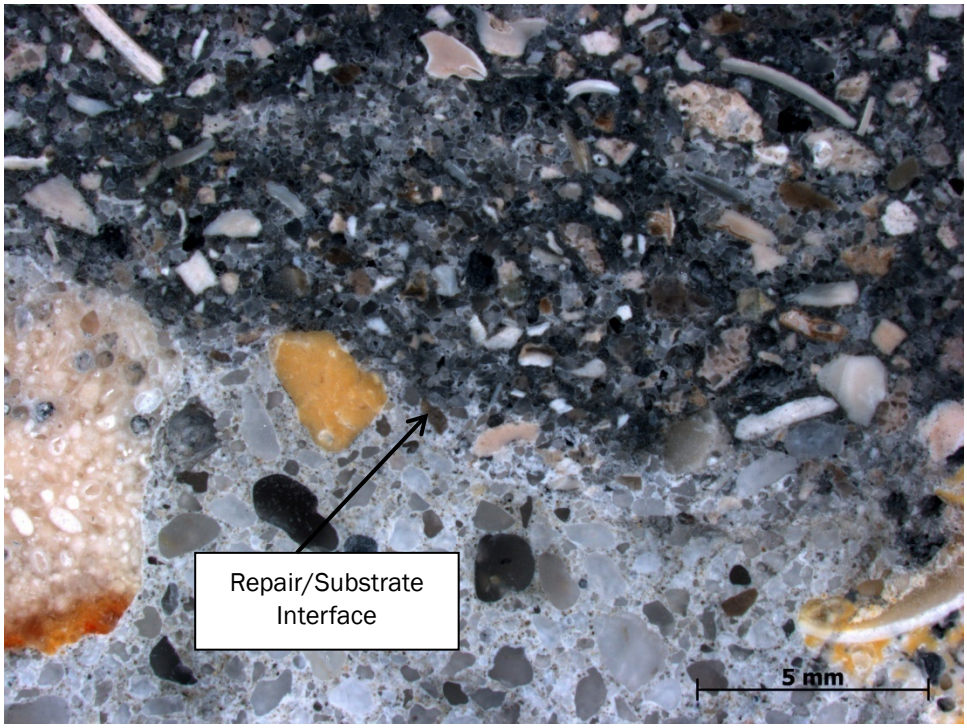

b. Typical repair interface #2.

Figure 10. Photomicrographs of typical deterioration in concrete from dam piers.

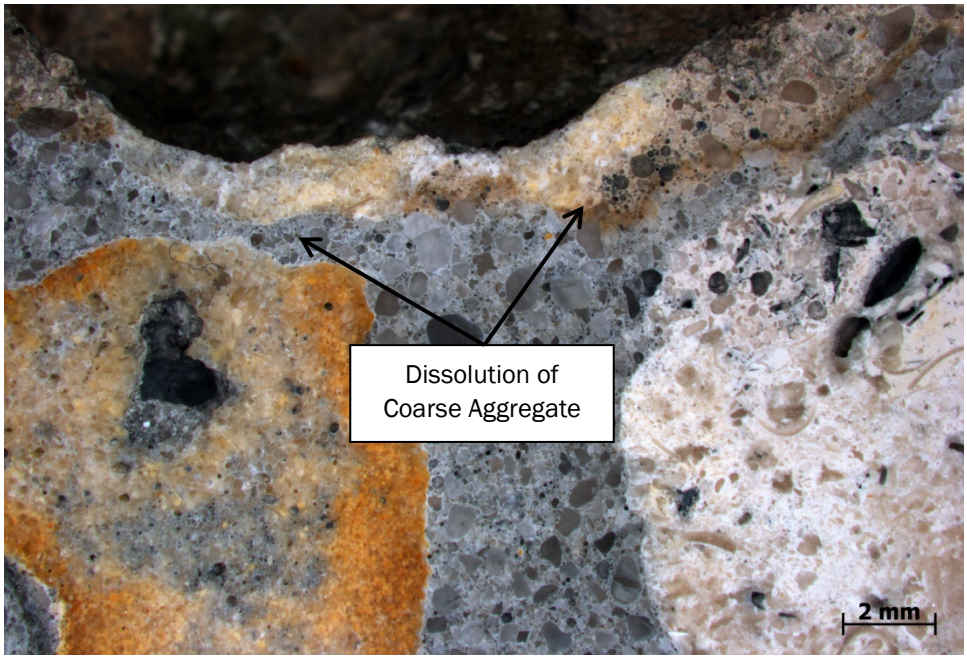

a. Low magnification photomicrograph.

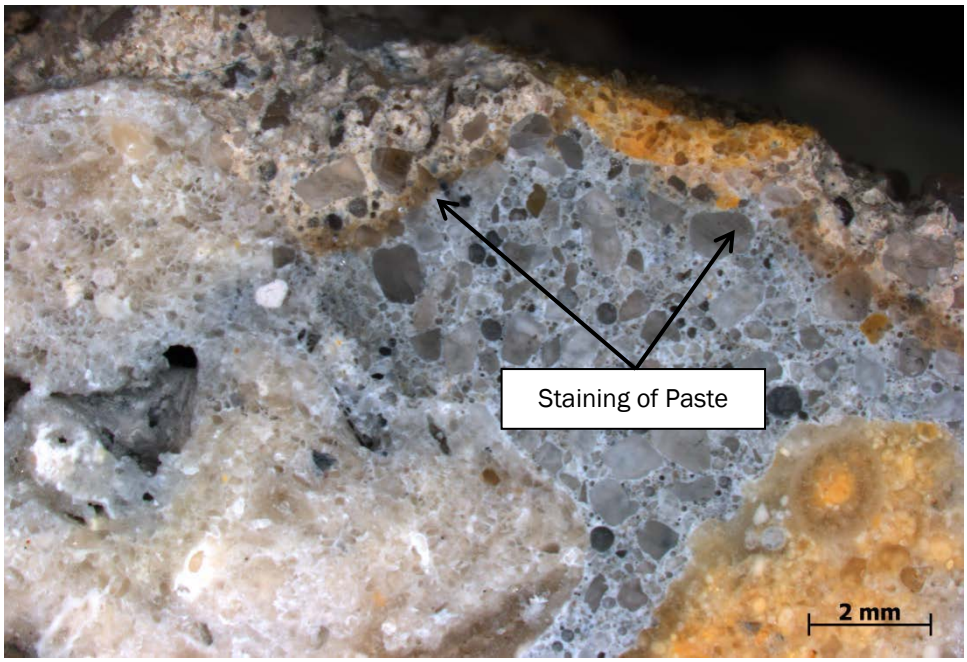

b. High magnification photomicrograph.

Figure 11. Photomicrographs of typical deterioration observed in concrete from lock chamber.

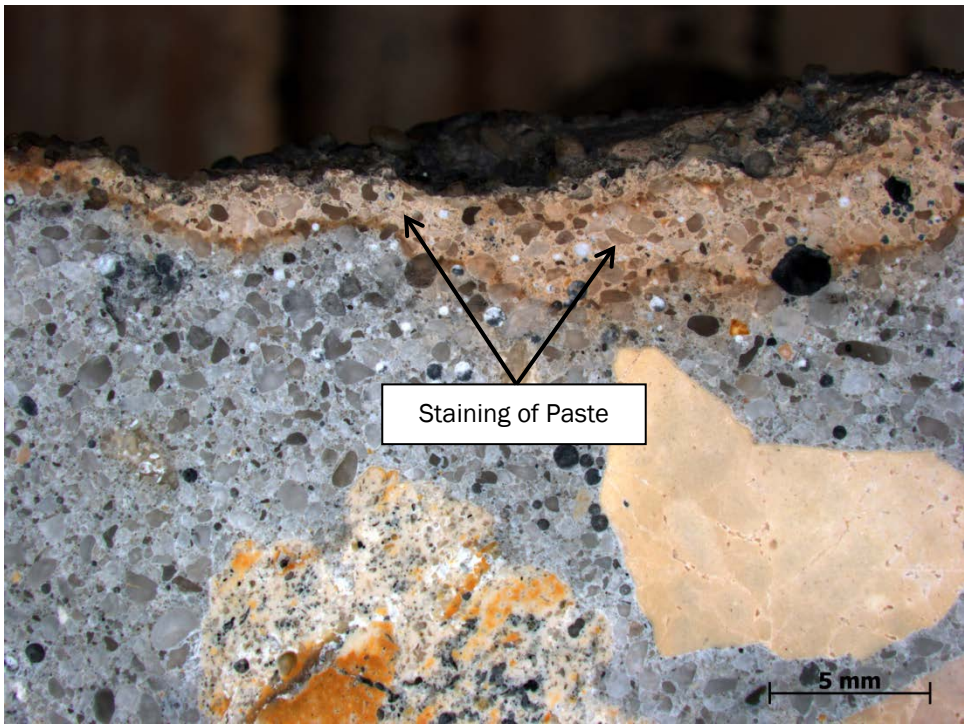

a. Low-magnification photomicrograph.

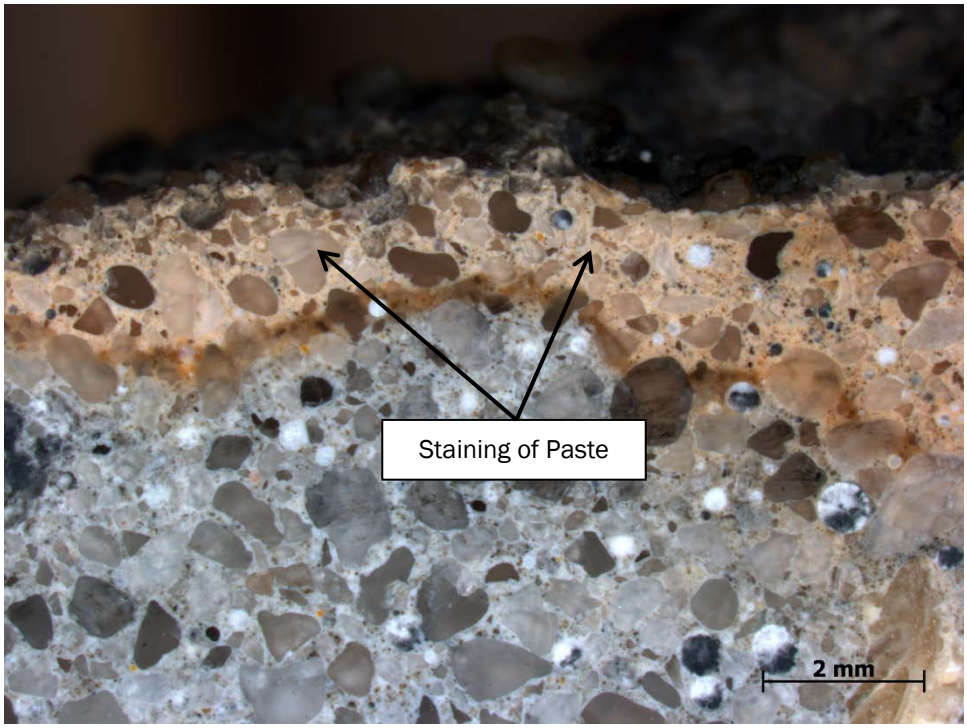

b. High-magnification photomicrograph.

In concrete from the dam and the lock, a surface layer of discolored concrete that is likely associated with acidification/carbonation (see Figure 12) or other forms of distress causing the surface deterioration were observed. Reduction in pH also appeared to be correlated with staining and the location of significant surface damage of the concrete. A borehole was also observed in one of the coarse aggregates, which was associated with the acidification front (see Figure 12). The deterioration was observed to focus primarily on the Pleistocene limestone aggregates and to a lesser extent on the hydrated cement paste itself. High magnification imaging of the surface concrete showed that the siliceous fine aggregates were largely unaffected by the surface deterioration (see Figures 13 and 14).

Based on water quality measurements, a lack of softening or spalling of the near surface concrete and the propensity of deterioration to focus on the Pleistocene limestone coarse aggregates and paste fraction of the concrete, it is unlikely that the distress results from sulfate attack or acid attack. No rust staining or microcracking was observed, which would be evidence of corrosion of the embedded reinforcing steel and would corroborate the low Cl^- concentrations measured in the water at S65E. A possible mechanism responsible for the observed distress is some form of biodeterioration, which has been previously observed in coastal and inland concrete structures. Biodeterioration may result in local acidification of the surface concrete, which would result in dissolution of limestone aggregates and decalcification of the paste but would have limited effect on siliceous fine aggregates. The aggregates and paste may also function as a direct food source for the biota with no acidification present. A second mechanism could be inorganic dissolution of limestone aggregate in contact with surface water having low carbonate alkalinity, as is typical in the Kissimmee River. This mechanism could explain limestone aggregate dissolution under neutral pH conditions.

Additional supplemental photomicrographs are in Appendix A.

3.3 X-ray diffraction analysis

XRD measurements were performed to determine the mineralogy of various phases present in the concrete and the differences between non-deteriorated bulk concrete and deteriorated surface concrete. Figure 15 shows typical XRD patterns of various constituents and regions investigated: coarse aggregate, fine aggregate, hydrated cement paste, bulk-deteriorated concrete, and deteriorated exposed concrete. Phases qualitatively identified to be present are shown at the bottom of Figure 15.

Figure 12. Acidifcation/carbonation depth of surface concrete evidenced by pH indicator. A borehole likely caused by biodeterioration was also observed.

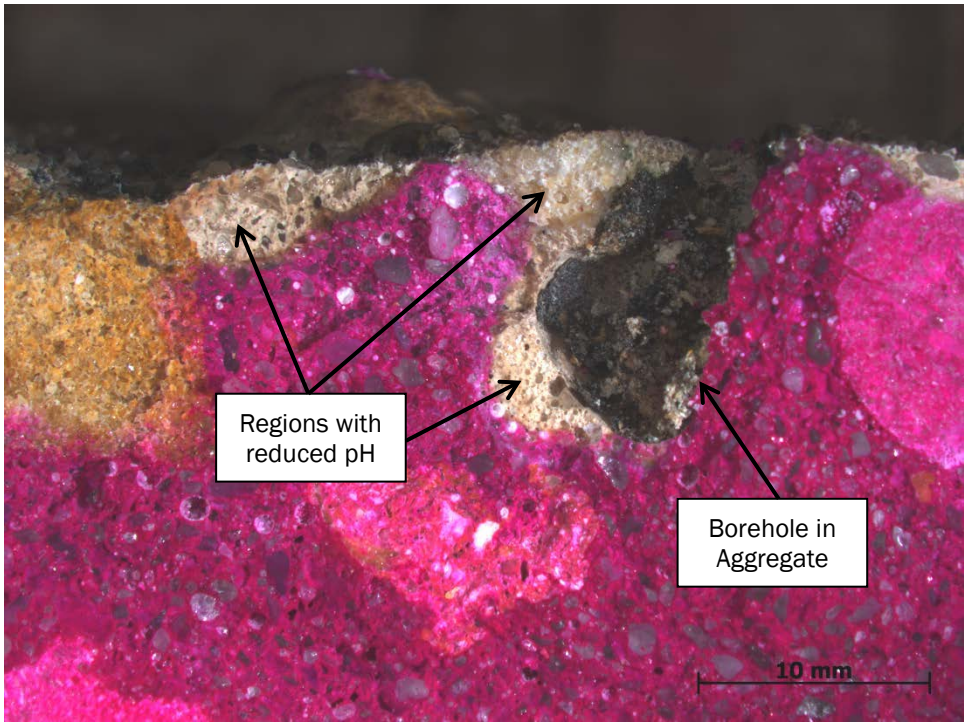

Figure 13. Photomicrograph of polished cross section of exposed concrete showing limited deterioration of siliceous fine aggregates when compared with limestone coarse aggregates and paste in exposed areas.

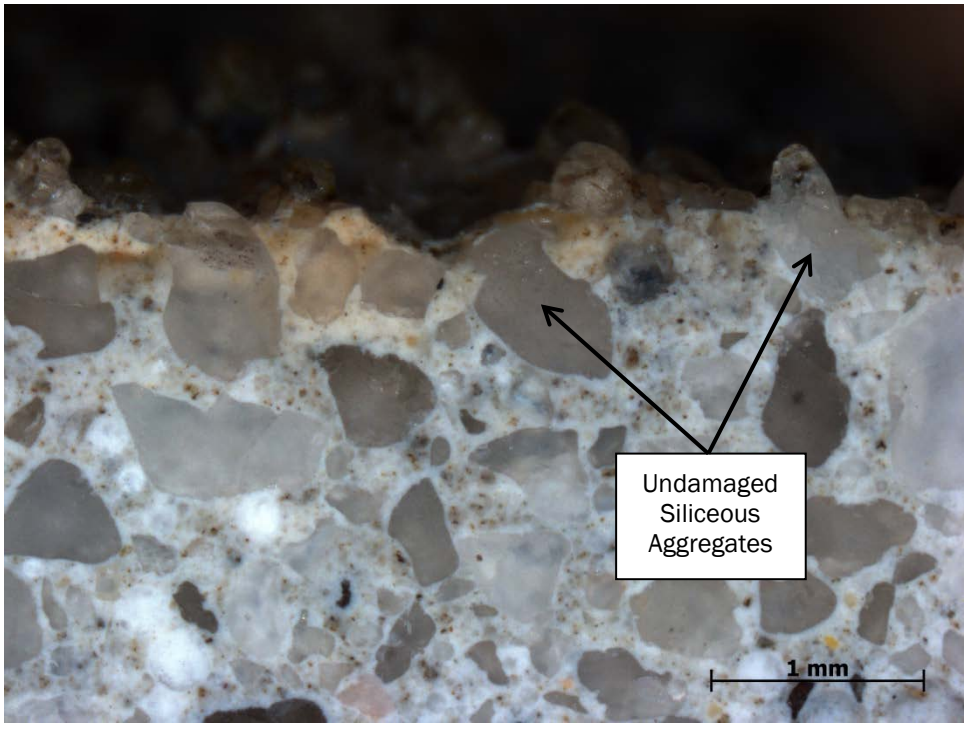

Figure 14. Photomicrograph of exposed surface of concrete showing biofilm growth and lack of damage to siliceous fine aggregates that remain exposed.

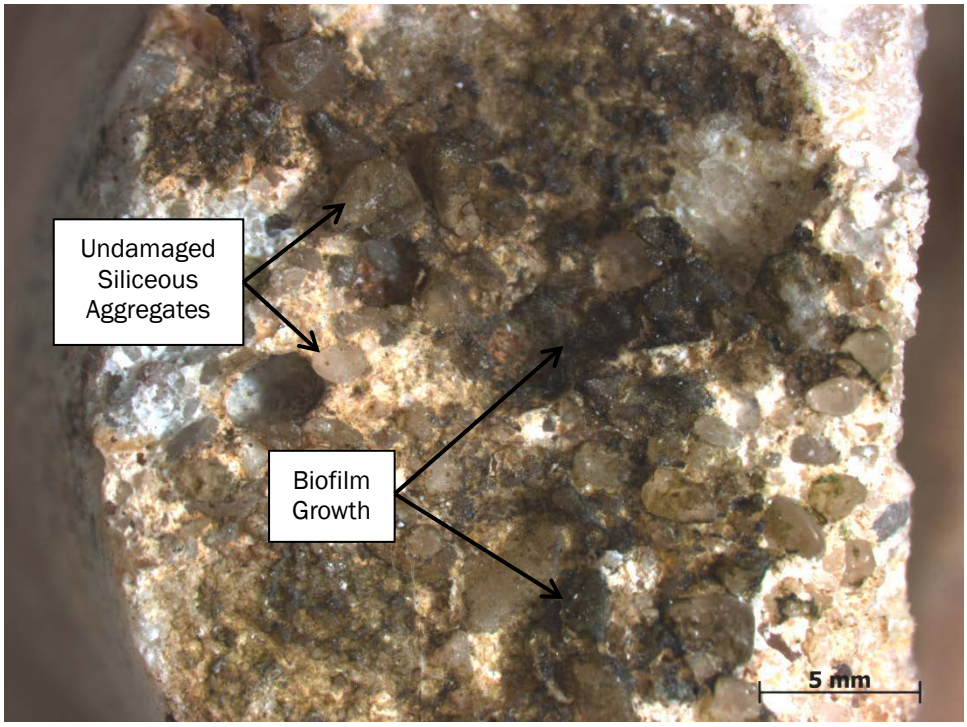

Figure 15. XRD patterns for non-deteriorated bulk concrete, exposed deteriorated concrete, coarse aggregates, fine aggregates, and hydrated cement paste with phases qualitatively identified as shown at the bottom of the plot and corresponding to the peak location in XRD pattern.

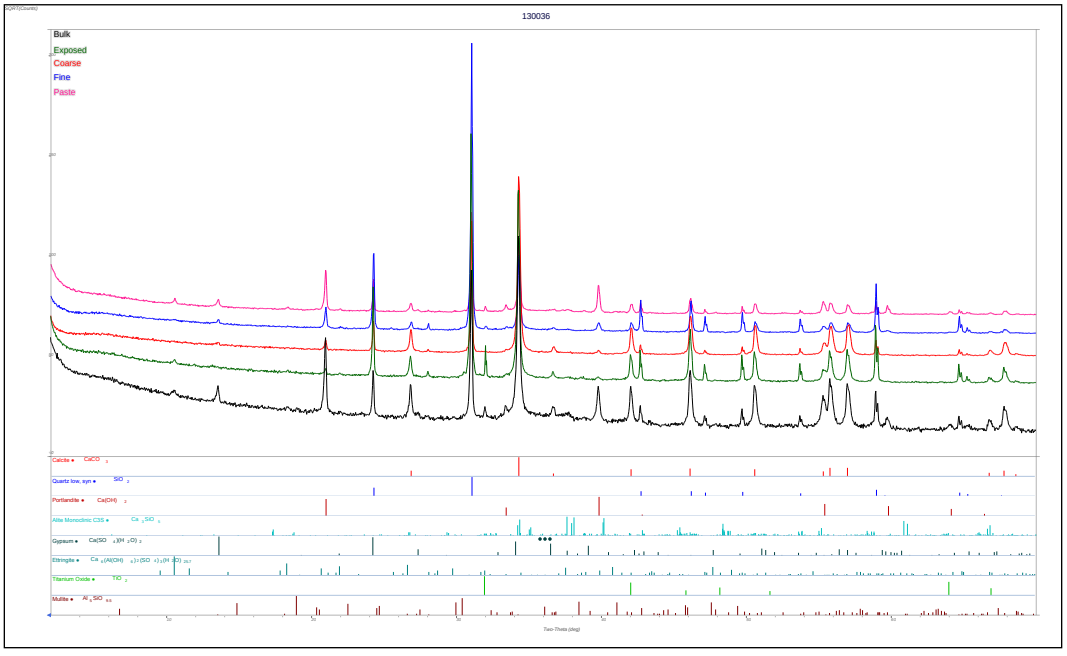

As anticipated, the coarse aggregate was primarily composed of Pleistocene limestone, containing the calcite polymorph of $CaCO_3$. The fine aggregate was primarily siliceous, containing the quartz polymorph of SiO_2. The paste has additional phases resulting from cement hydration, including ettringite and portlandite, along with unreacted gypsum and alite (C_3S) contributed by portland cement.

The most useful comparisons can be made between the bulk non-deteriorated concrete and the surface deteriorated concrete. Figure 16 presents the results of quantitative whole pattern fitting of samples from bulk non-deteriorated concrete and surface deteriorated concrete.

Figure 16. Results from quantitative XRD whole pattern fitting from bulk concrete and surface concrete from exposed areas that exhibited deterioration.

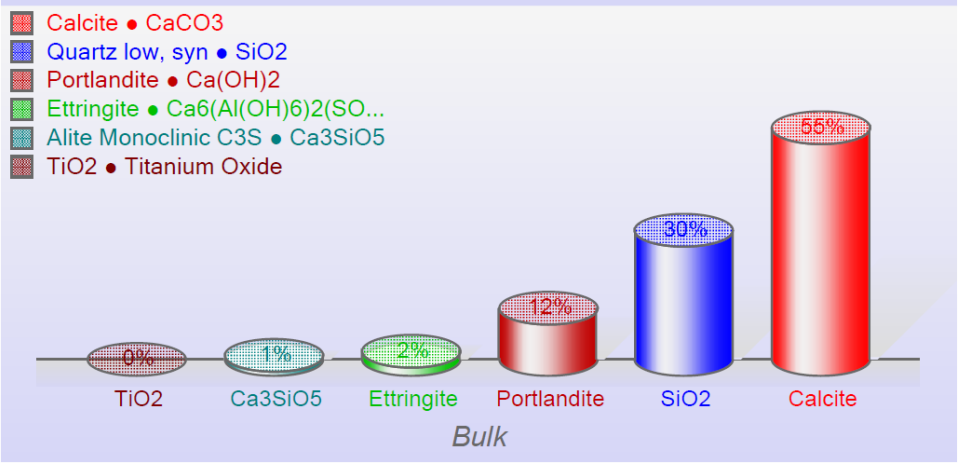

a. Quantitative analysis results from bulk non-deteriorated concrete.

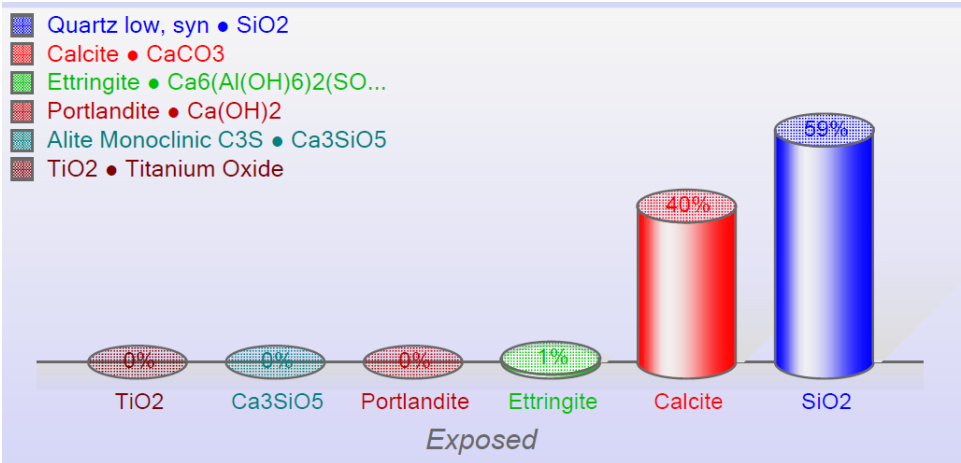

b. Quantitative analysis results from surface deteriorated concrete.

In the case of the bulk non-deteriorated concrete, calcite, associated with coarse aggregates, and quartz (SiO_2), associated with fine aggregates, dominated the composition, followed by cement hydration products portlandite ($Ca(OH)_2$) and ettringite ($\sim Ca_6(Al(OH)_2)_2(SO_4)_3(H_2O)_{25}$), along with residual unhydrated cement (Alite/C_3S). In the surface deteriorated concrete, significantly more quartz was present from undamaged fine aggregates, and less calcite was present from the deterioration of Pleistocene coarse aggregates. A reduction in soluble hydrates including portlandite and ettringite occurred. The loss of portlandite and ettringite at the surface is typical for leaching of these highly soluble phases in high-moisture environments. The lack of ettringite or other phases typically present in concrete damaged by sulfate attack such as gypsum supports our hypothesis that sulfate attack is likely not a concern, as SO_4^{2-} concentrations are low in the local water at S65E. The reduction in calcite and increase in quartz composition at the surface also supports the hypothesis that biodeterioration may be leading to distress by consumption of limestone coarse aggregates and the paste. However, this finding is highly related to the location of sampling on the concrete core.

3.4 Scanning electron microscopy

High-resolution imaging of deterioration at the surface of the concrete and also of the transition in deterioration from the surface to the inner bulk concrete was performed using scanning electron microscopy (SEM) of the as-received concrete surfaces and internal fracture surfaces. Typical SEM micrographs of the as-received surface of the deteriorated concrete are shown in Figure 17. The surface was highly populated by various biological species that were present primarily on the paste and limestone coarse aggregates. The biota appeared to consist of some type of bio-film along with diatom-like structures.

Further investigation of the surface showed a clear distinction between deterioration of limestone coarse aggregates and siliceous fine aggregates. Figure 18 shows an example of deterioration observed on the as-received concrete surface, with biological growth focused on paste and limestone aggregates; an unaffected fine aggregate; and apparent dissolution of an exposed portion of a limestone coarse aggregate. The dissolution of the limestone appeared to be correlated with the rhombohedral structure of calcite and changed with grain orientation in the coarse aggregate.

Figure 17. SEM micrographs of as-received deteriorated concrete surface showing biological growth present.

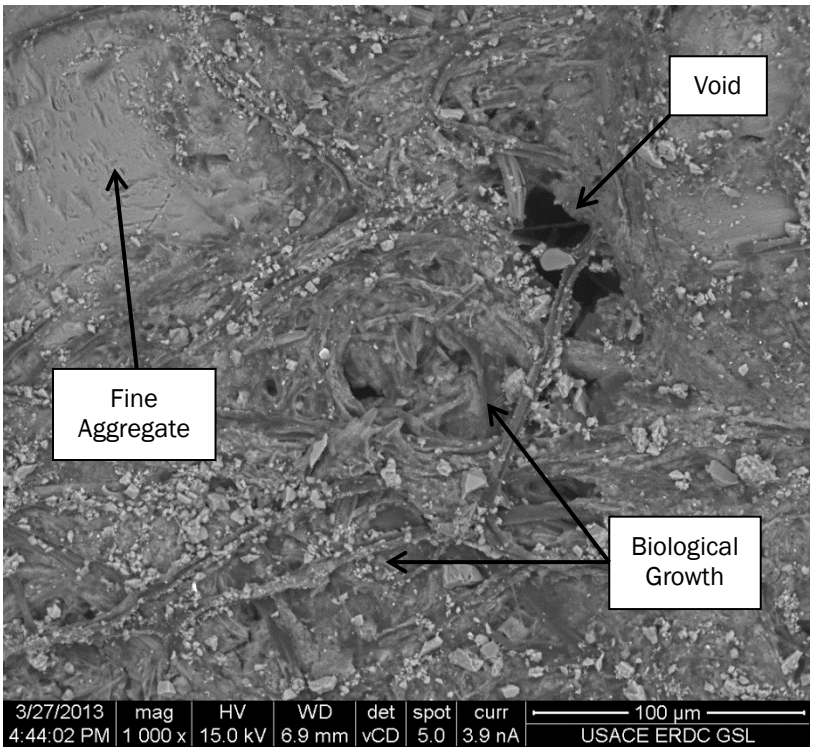

a. Quantitative analysis results from bulk non-deteriorated concrete.

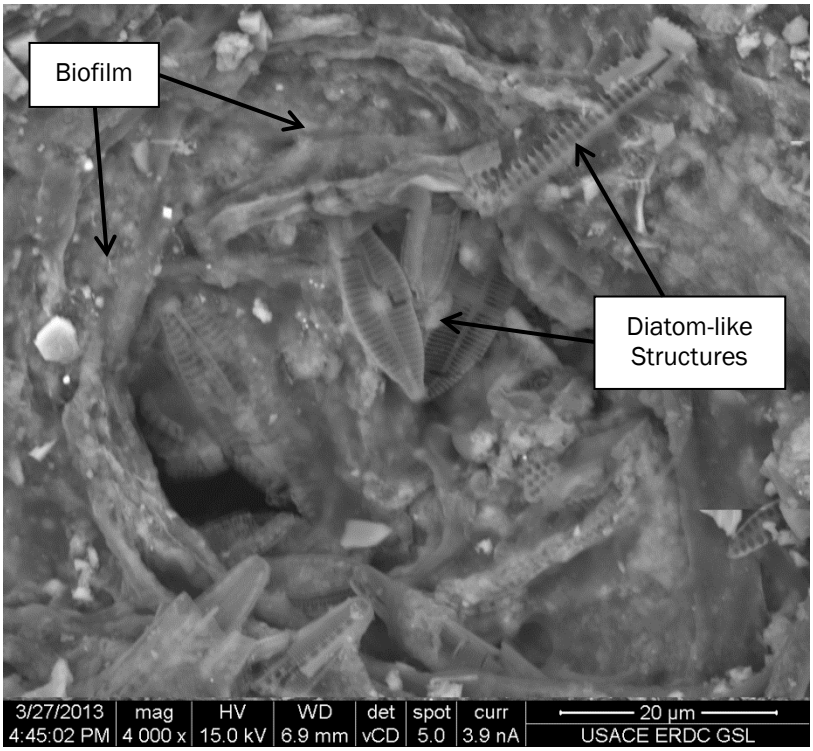

b. Quantitative analysis results from surface deteriorated concrete.

Figure 18. Progression in damage observed on as-received deteriorated concrete surface showing biological growth, unaffected siliceous fine aggregate, and dissolution of limestone coarse aggregate. Red boxes identify "zoomed in" areas in subsequent images.

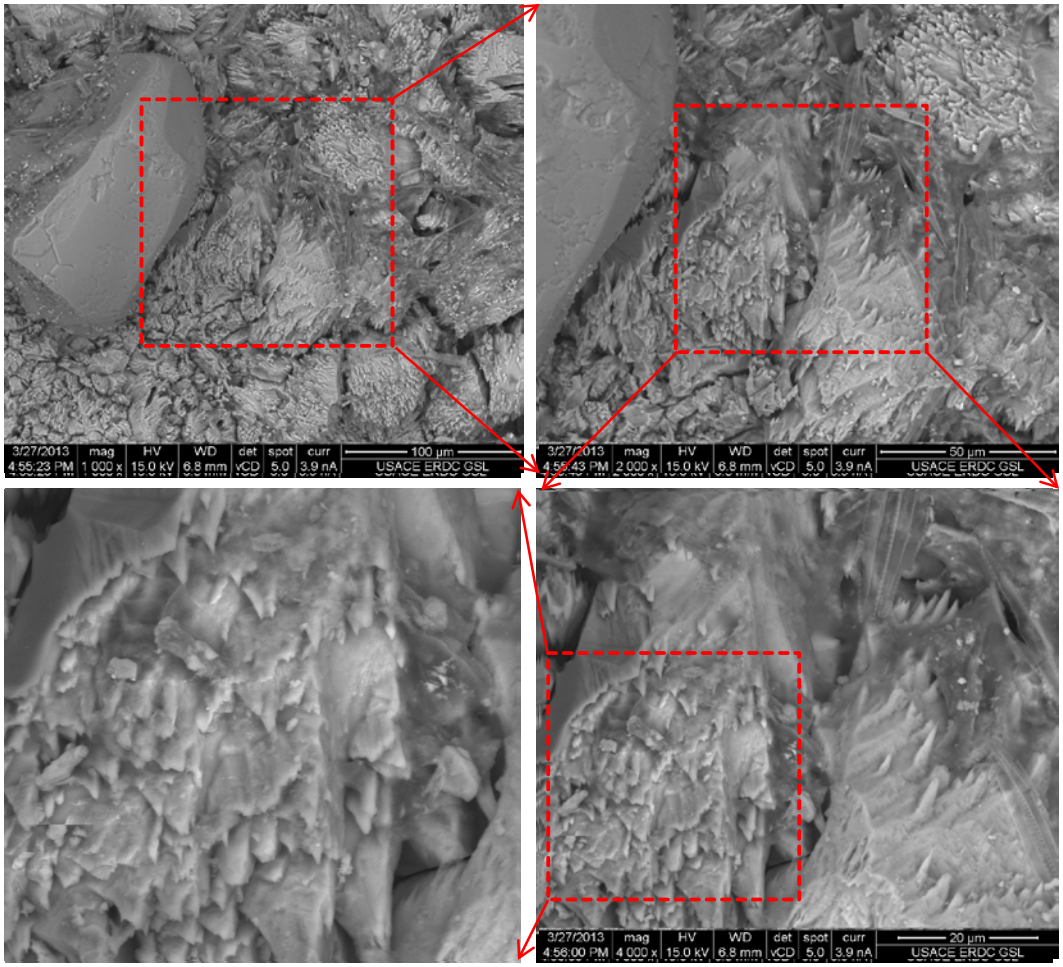

Further examination of microcores extracted from the surface and split longitudinally was used to investigate damage from the surface in. Figure 19 shows examples of deterioration observed on the fracture surface and the transition between the surface deterioration and the non-deteriorated bulk concrete and unaffected aggregates. The inner bulk concrete appeared typical with no detectable other modes of deterioration (see Figure 20).

Figure 19. SEM micrographs of deterioration observed on fracture surface including borehole near exposed surface and transition between deteriorated and non-deteriorated limestone in Pleistocene limestone coarse aggregate.

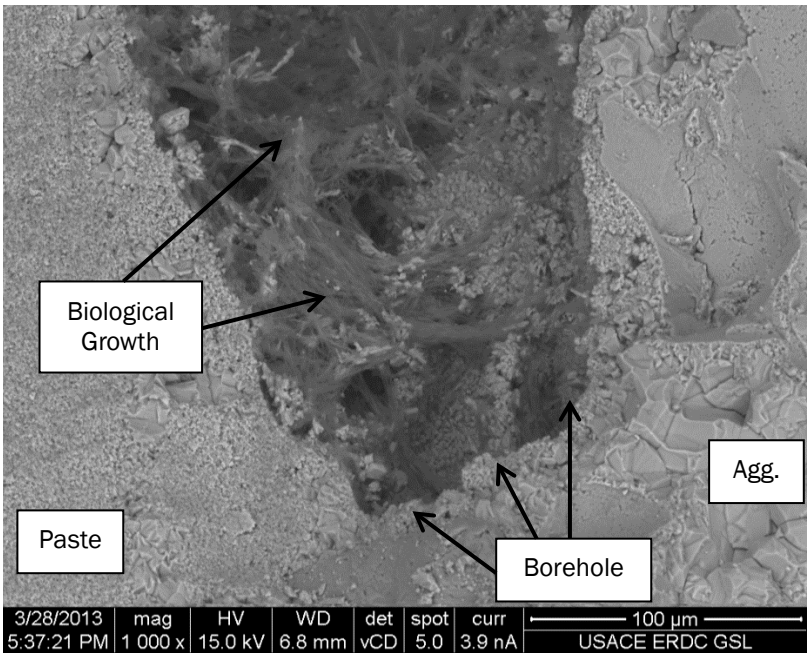

a. Deterioration and borehole observed on fracture surface.

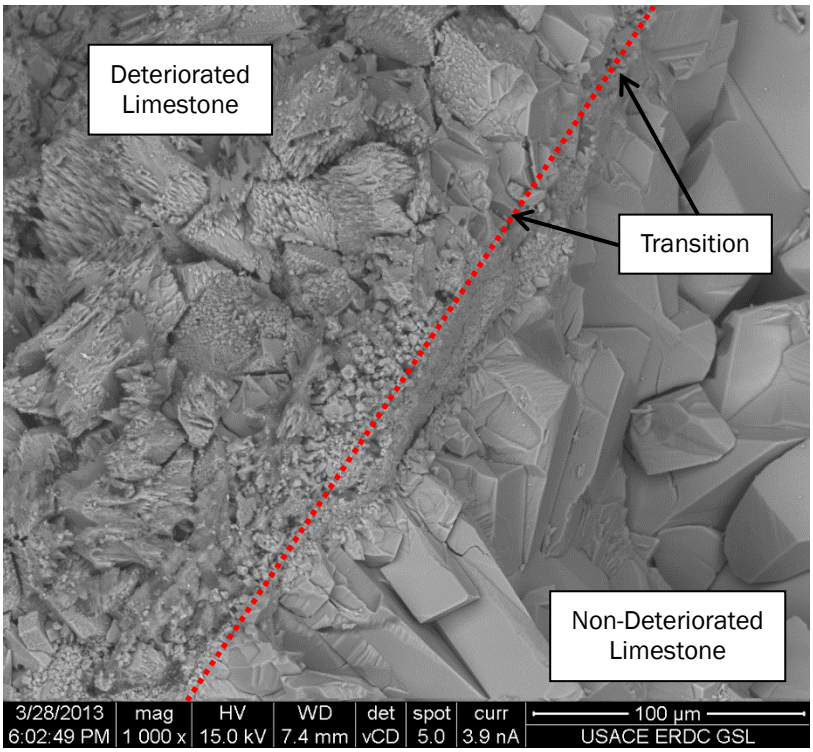

b. Transition between deteriorated and non-deteriorated limestone.

Figure 20. SEM micrographs of inner bulk non-deteriorated concrete showing typical distribution in paste, fine aggregates, and the Pleistocene limestone coarse aggregate.

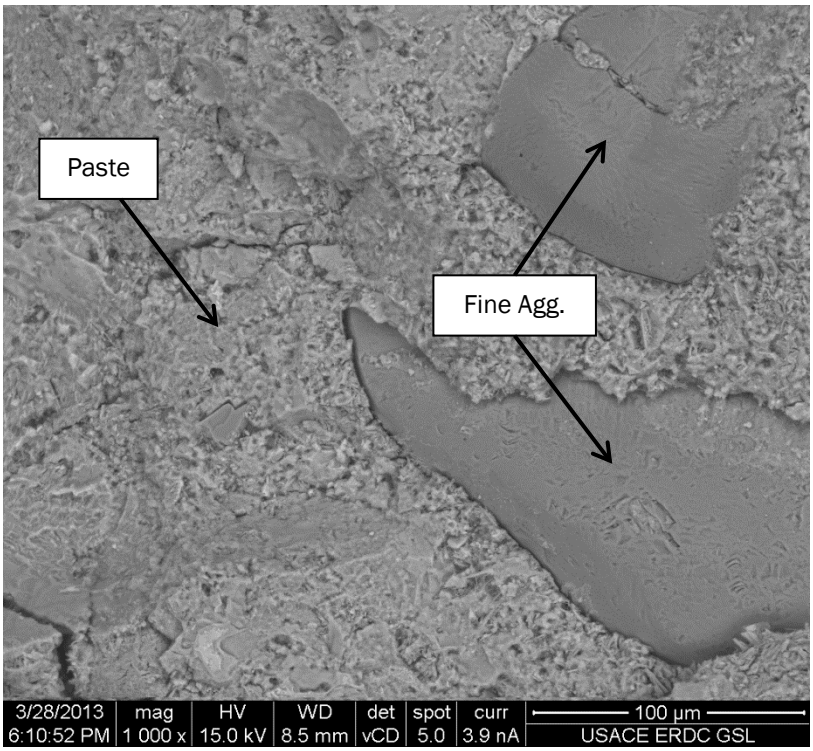

a. Fracture surface of bulk concrete showing paste and fine aggregate.

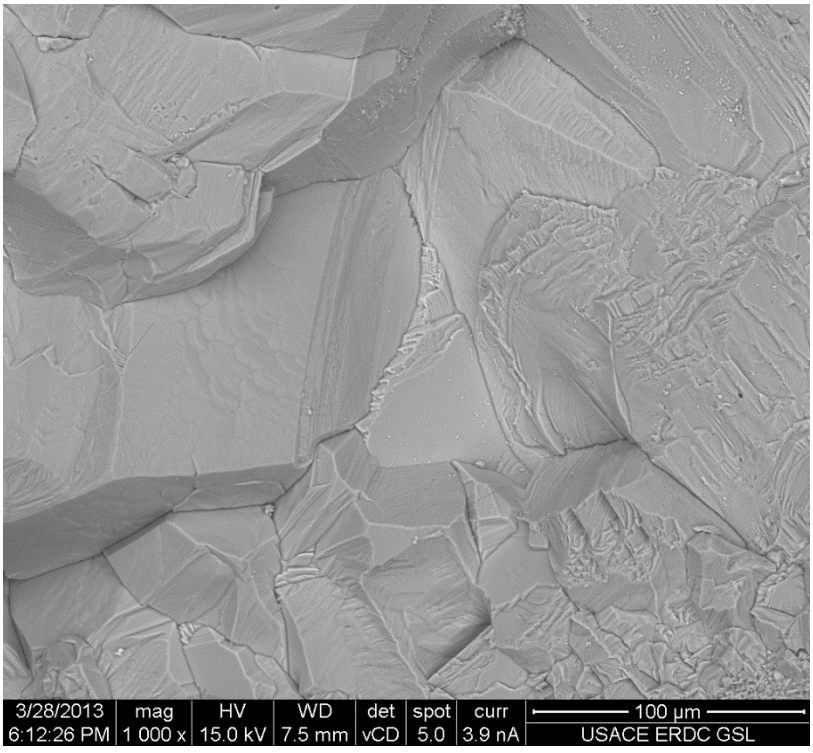

b. Fracture surface of non-deteriorated limestone coarse aggregate.

Results of the SEM investigations confirmed that the deterioration observed in concrete from the lock chamber and dam at S65E is largely concentrated on the surface. Deterioration observed at the surface appeared to be correlated with biological activity and active dissolution of soluble components present in the concrete, as indicated by geochemical water-rock reaction simulations. Dissolution of the paste and limestone coarse aggregates was observed, while the siliceous fine aggregates appeared to be relatively unaffected. Deterioration was correlated with the depth of discoloration observed by petrographic analysis and reported in Section 3.2. The inner bulk concrete did not appear to have any type of detectable deterioration (e.g., sulfate attack or biodeterioration of the paste, coarse aggregate, and fine aggregate).

Additional supplemental SEM micrographs are in Appendix B.

4 Summary, Conclusions, and Recommendations

This report documents the findings of a concrete deterioration study of South Florida Water Management District (SFWMD) Structure S65E. The research was coordinated in support of the Jacksonville District which is working in collaboration with the SFWMD. ERDC personnel in the Concrete and Materials Branch of the Geotechnical and Structures Laboratory provided technical assistance in the forensic examination of the concrete. The study examined water quality at the S65E site and concrete cores from deteriorated, repaired, and non-deteriorated areas of the structure. A total of seven concrete cores were received by ERDC for analysis. Geochemical water-rock reaction simulations were also performed using historical water quality data to assess the potential for active dissolution of various components present in the concrete.

The predominant form of deterioration observed was severe loss of both paste and Pleistocene limestone coarse aggregates from the surface of the concrete, with larger losses in high-flow rate areas of the dam piers than in low-flow rate areas of the lock chamber. The siliceous fine aggregates appeared to be unaffected. Water quality analysis found negligible concentrations of SO_4^{2-} and Cl^- and a neutral pH of approximately 7. Water-rock interaction modelling showed that coarse limestone aggregate, as represented by the minerals calcite and dolomite, will deteriorate by inorganic dissolution in contact with Kissimmee River surface water. Water-rock interaction modelling showed that coarse limestone aggregate is stable and will not dissolve in contact with C-51 surface water at S-5A. Lack of concrete deterioration at structures located south of Lake Okeechobee is consistent with surface water quality that has a greater buffering capacity, a higher total carbonate alkalinity, and a neutral-to-slightly-alkaline pH.

X-ray diffraction analysis of various components (i.e., paste, coarse aggregate, and fine aggregate) and regions in the concrete (i.e., inner bulk and exposed surface) showed evidence of minor carbonation and leaching of soluble phases from the surface of the concrete but no evidence of deterioration resulting from sulfate attack. Petrographic analysis of concrete from non-deteriorated areas showed minor carbonation but no other detectable deterioration. Concrete from deteriorated areas exhibited

significant loss of Pleistocene limestone coarse aggregates and paste while the siliceous fine aggregates were unaffected. The shotcrete repair material appeared to have a good bond with the concrete substrate but was extremely porous and also contained the same limestone aggregates that were found to be prone to deterioration in the original concrete at S65E. High magnification photomicrographs obtained using SEM confirmed dissolution of the limestone coarse aggregates at the surface, while siliceous fine aggregates were unaffected. Select bore holes infilled with biological growth were also observed near the exposed surface. These results suggest that sulfate attack, acid attack, Cl^- induced corrosion, or other typical forms of concrete deterioration are likely not the cause(s) of the observed deterioration.

Biodeterioration can explain local deterioration at the surface by acidification and direct or chemical consumption of mineral phases present in concrete (e.g., $CaCO_3$). Similar modes of deterioration have recently been reported (see Figure 21). However, water-rock reaction simulations have also evidenced the potential for active dissolution of soluble components in the concrete (e.g., calcite and dolomite) based on the typical local water quality at S65E.

Regarding recommendations for the repair strategy, the shotcrete repair technique employed, while most simple, is likely not the most durable repair technique for wall rehabilitation, as it is more prone to cracking and delamination following application. Cast-in-place concrete, preplaced aggregate concrete, or retrofit with stay-in-place precast concrete panels are other options. Further information on lock wall rehabilitation can be obtained from the following:

- *Lock wall rehabilitation*, Engineer Manual 1110-2-2002, Section 8-1, USACE, and
- McDonald, J.E., *Rehabilitation of navigation lock walls: Case histories*, Technical Report REMR-CS-13, USAEWES.

Based on the results of this study, durability of the repair material (whether concrete, grout, or mortar) could likely be improved with the use of siliceous aggregates to minimize the deterioration observed in limestone aggregates in the existing concrete (note: biodeterioration mechanism must be validated). Efforts to minimize porosity/permeability (e.g., low w/cm, use of water-reducing admixtures, or addition of various supplementary

cementitious materials) and improve acid resistance (e.g., use of silica fume) would likely improve the durability of the repair material. The use of a high quality repair material that is durable will also serve to better protect the underlying concrete from subsequent deterioration.

Figure 21. Similar microbial-induced biodeterioration observed in Texas bridge structures exposed to environments similar to those at structure S65E (from Trejo 2008).

a. Example biodeterioration of concrete surface in Texas bridge structure.

b. Sampling locations for study of surface biodeterioration in Texas bridge structure.

References

Parkhurst, D. L., and C. A. J. Appelo. 1999. *User's guide to PHREEQC (version 2) – A computer program for speciation, batch-reaction, one-dimensional transport, and inverse geochemical calculations*. US Geological Survey (USGS) Water-Resources Investigations Report 99-4259, Reston, VA: USGS.

Trejo, D. 2008. *Analysis and assessment of microbial biofilm-mediated concrete deterioration*. College Station, TX: Southwest Region University Transportation Center.

Appendix A: Supplemental Photomicrographs

Figure A1. Supplemental photomicrographs of bulk non-deteriorated concrete.

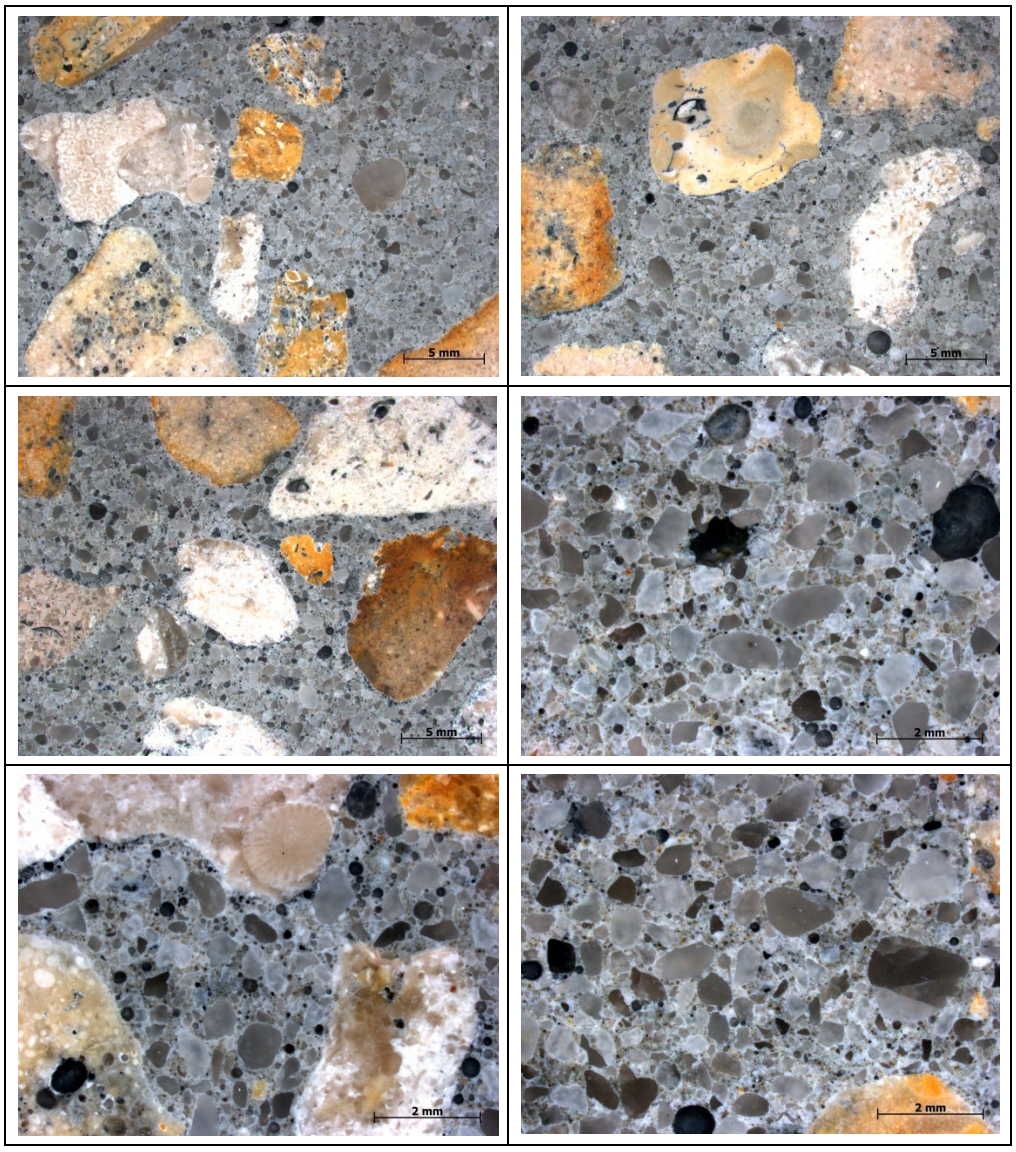

Figure A2. Supplemental photomicrographs of deteriorated concrete from core D2.

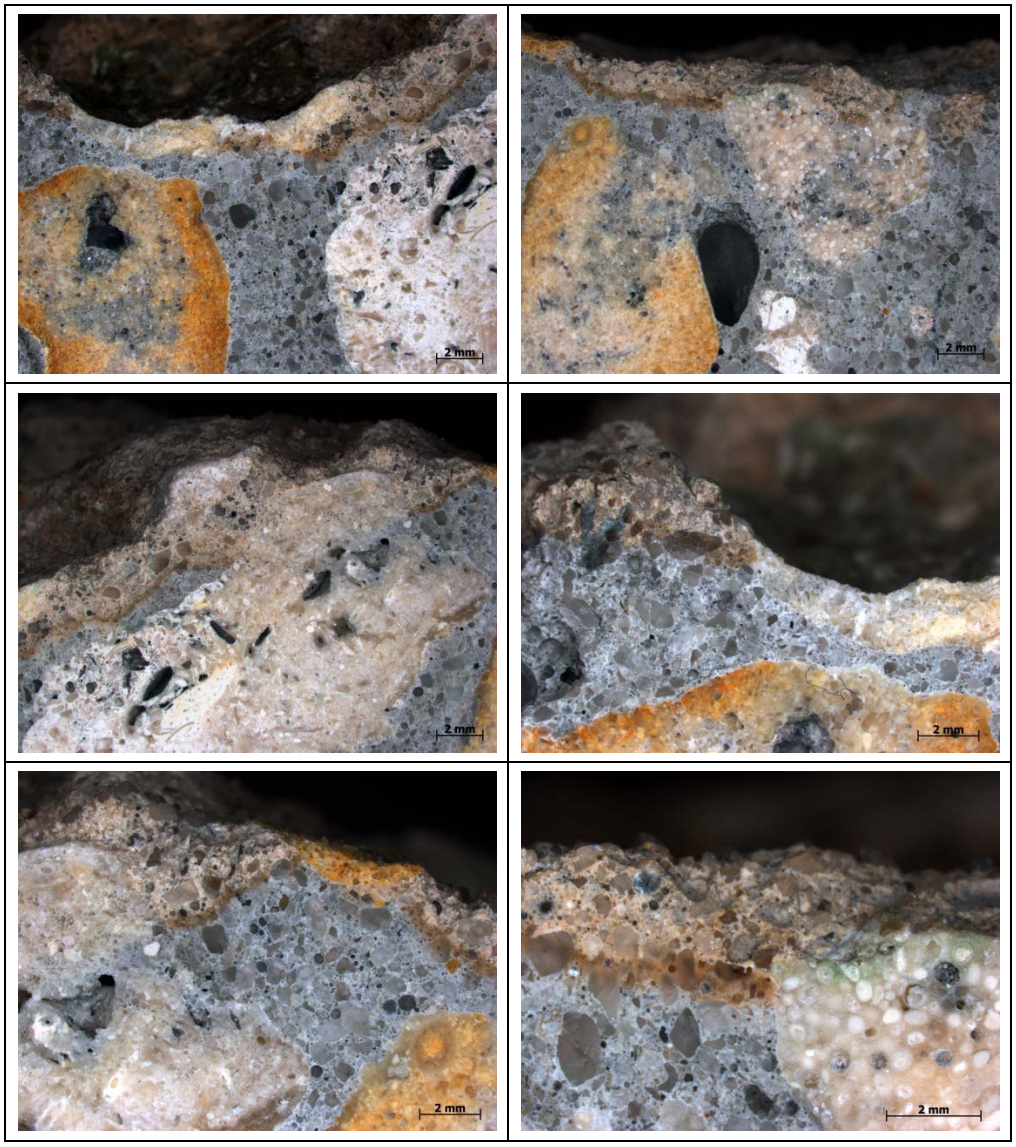

Figure A3. Supplemental photomicrographs of deteriorated concrete from core D3.

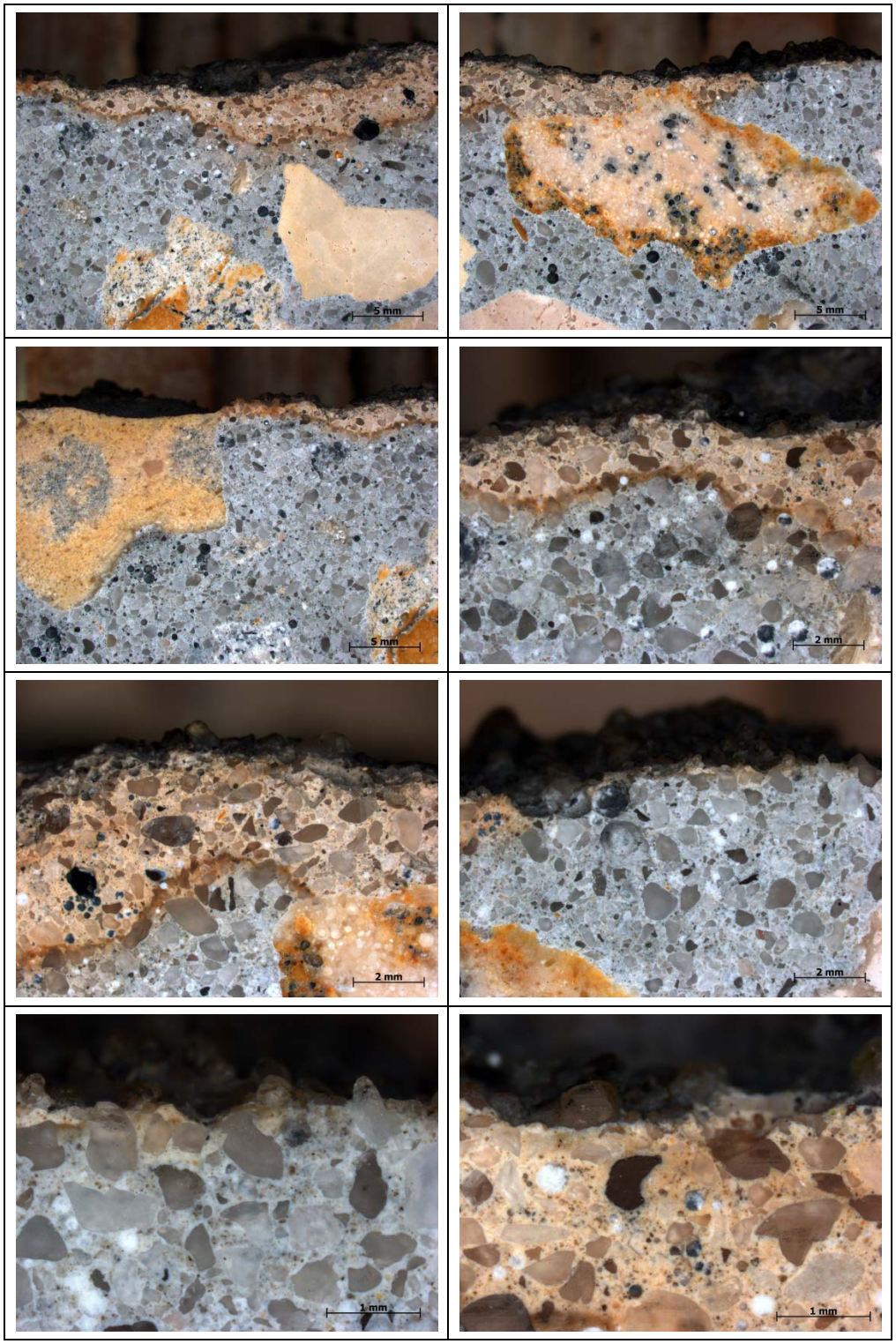

Figure A4. Supplemental photomicrographs of non-deteriorated concrete surface.

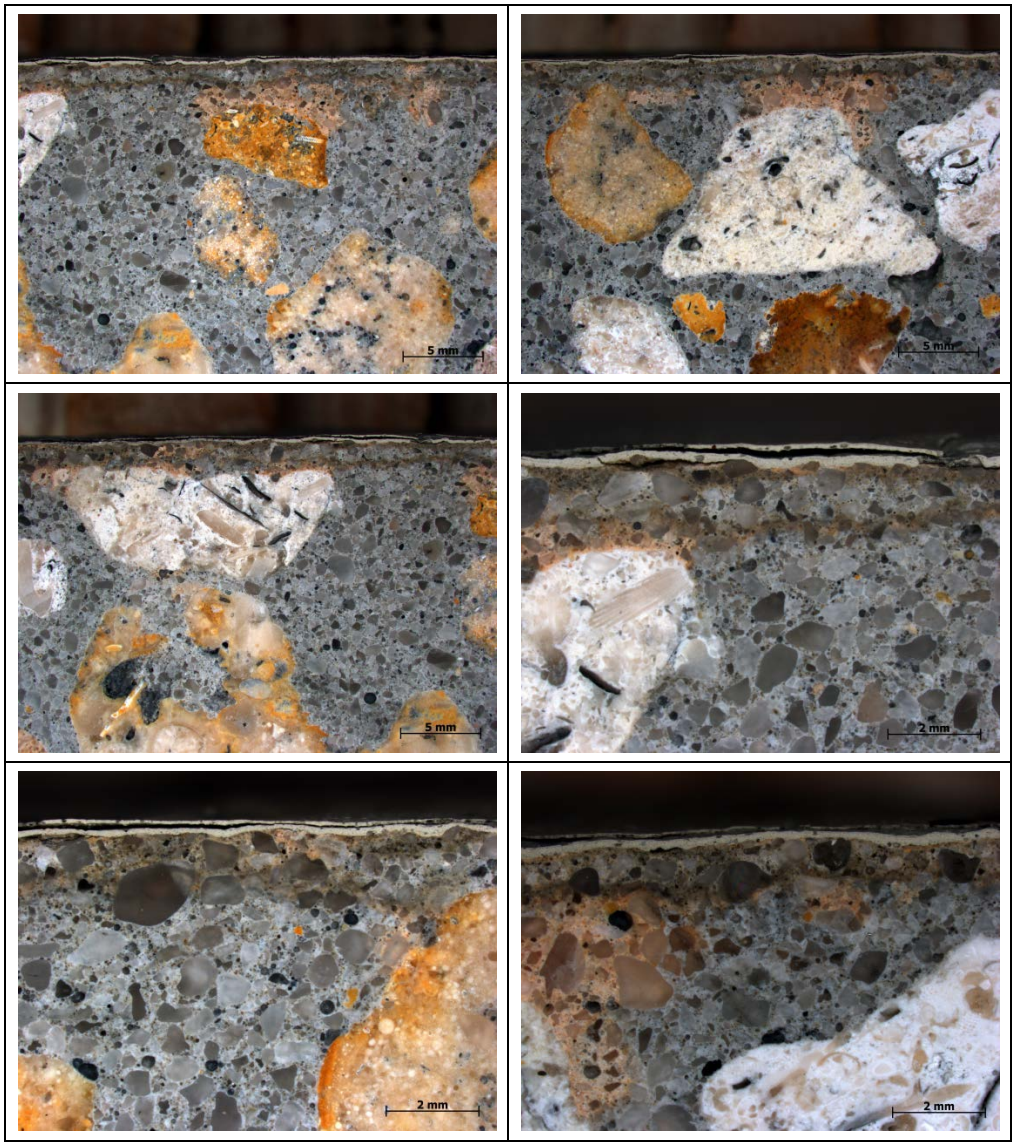

Figure A5. Supplemental photomicrographs of repaired concrete surface.

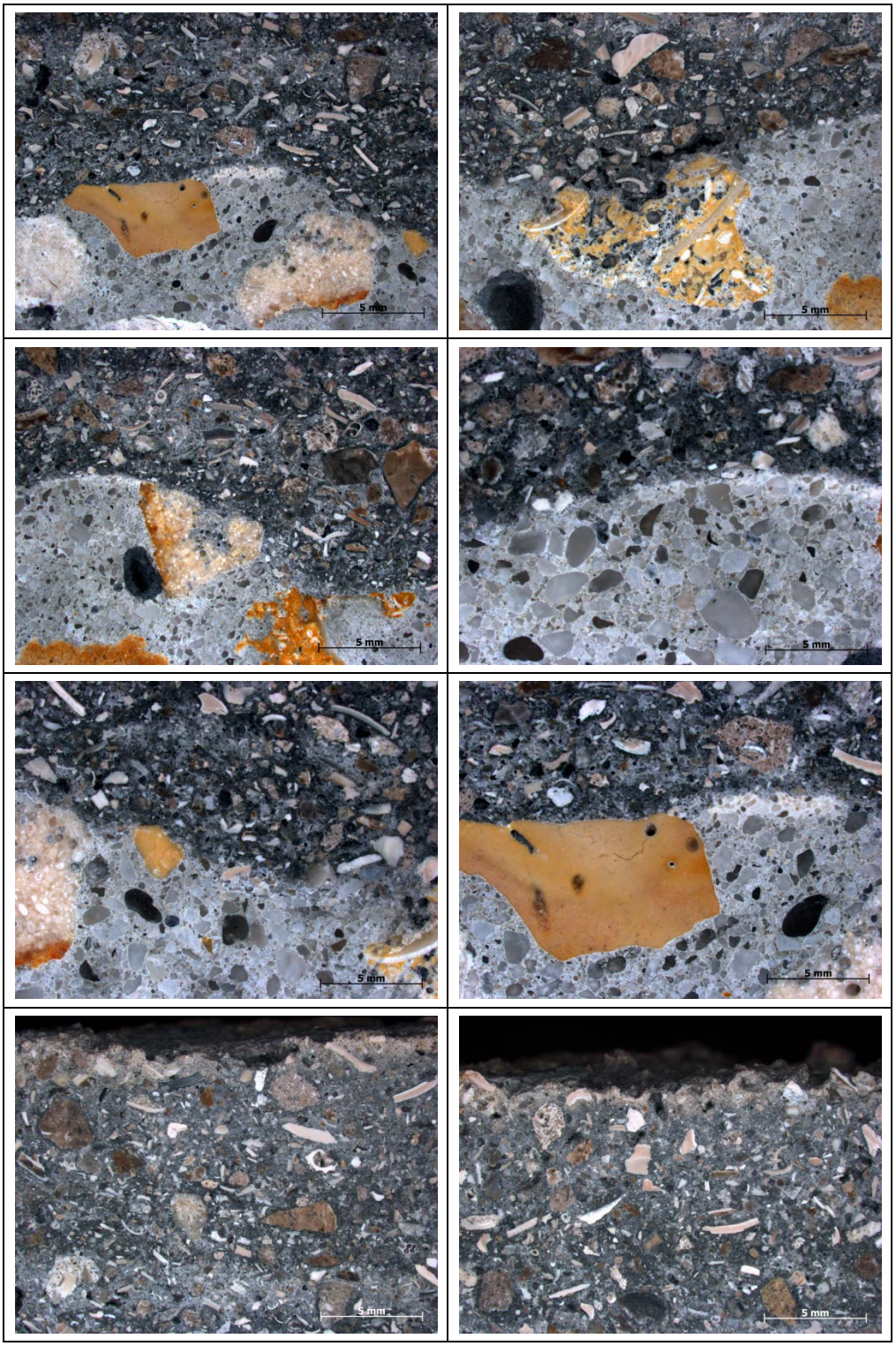

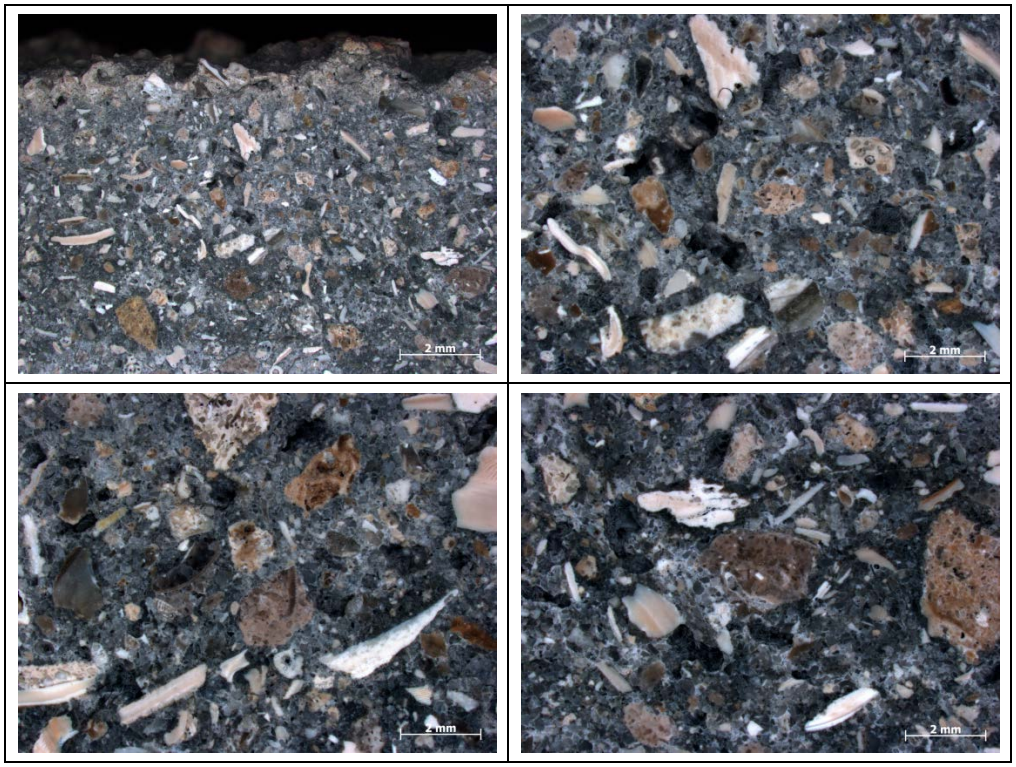
2 mm
2 mm
2 mm
2 mm

Figure A6. Supplemental photomicrographs of fractured sample of concrete, including deteriorated surface.

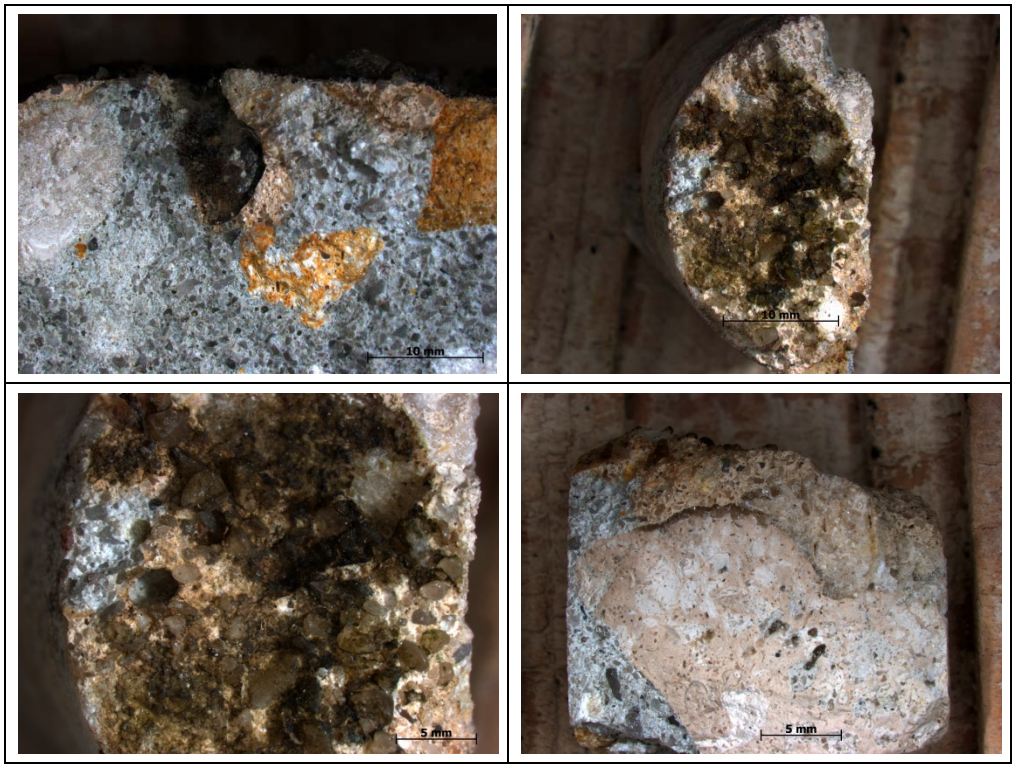

Appendix B: Supplemental SEM Micrographs

Figure B1. Supplemental SEM micrographs of inner non-deteriorated concrete fracture surface.

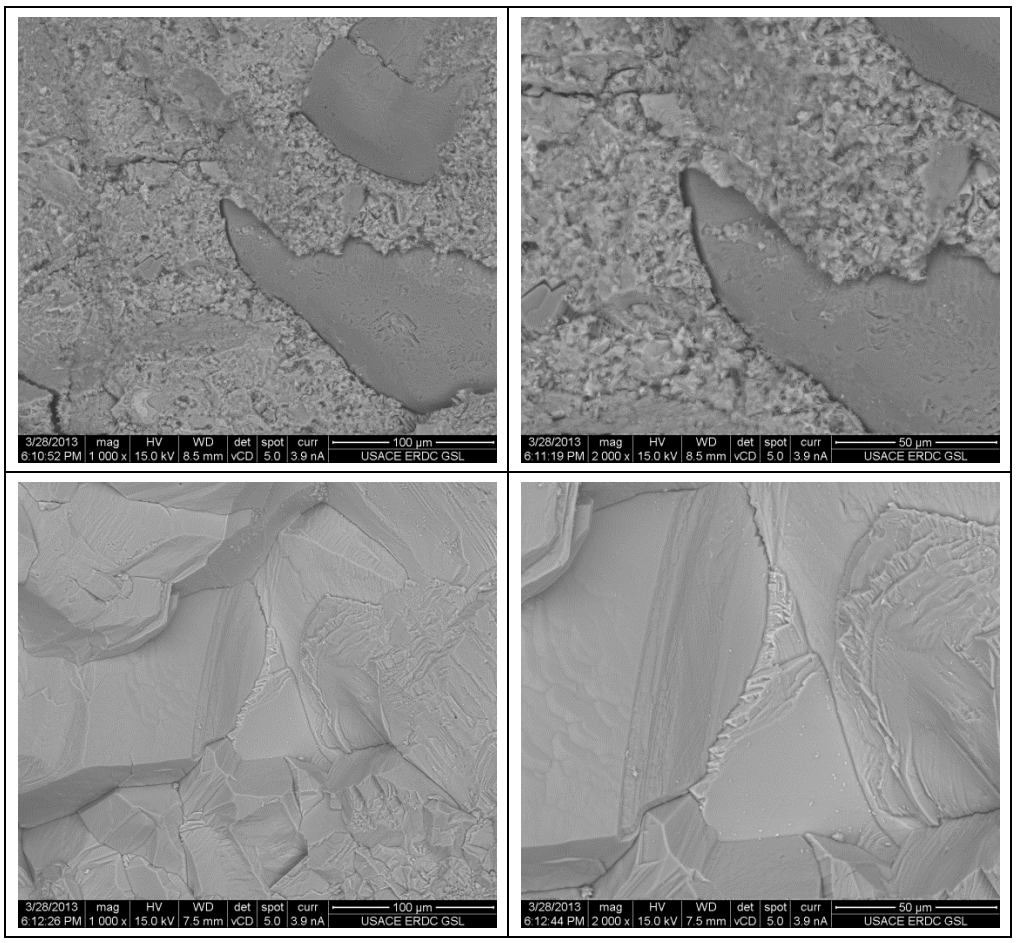

Figure B2. Supplemental SEM micrographs of fractured surface of deteriorated concrete.

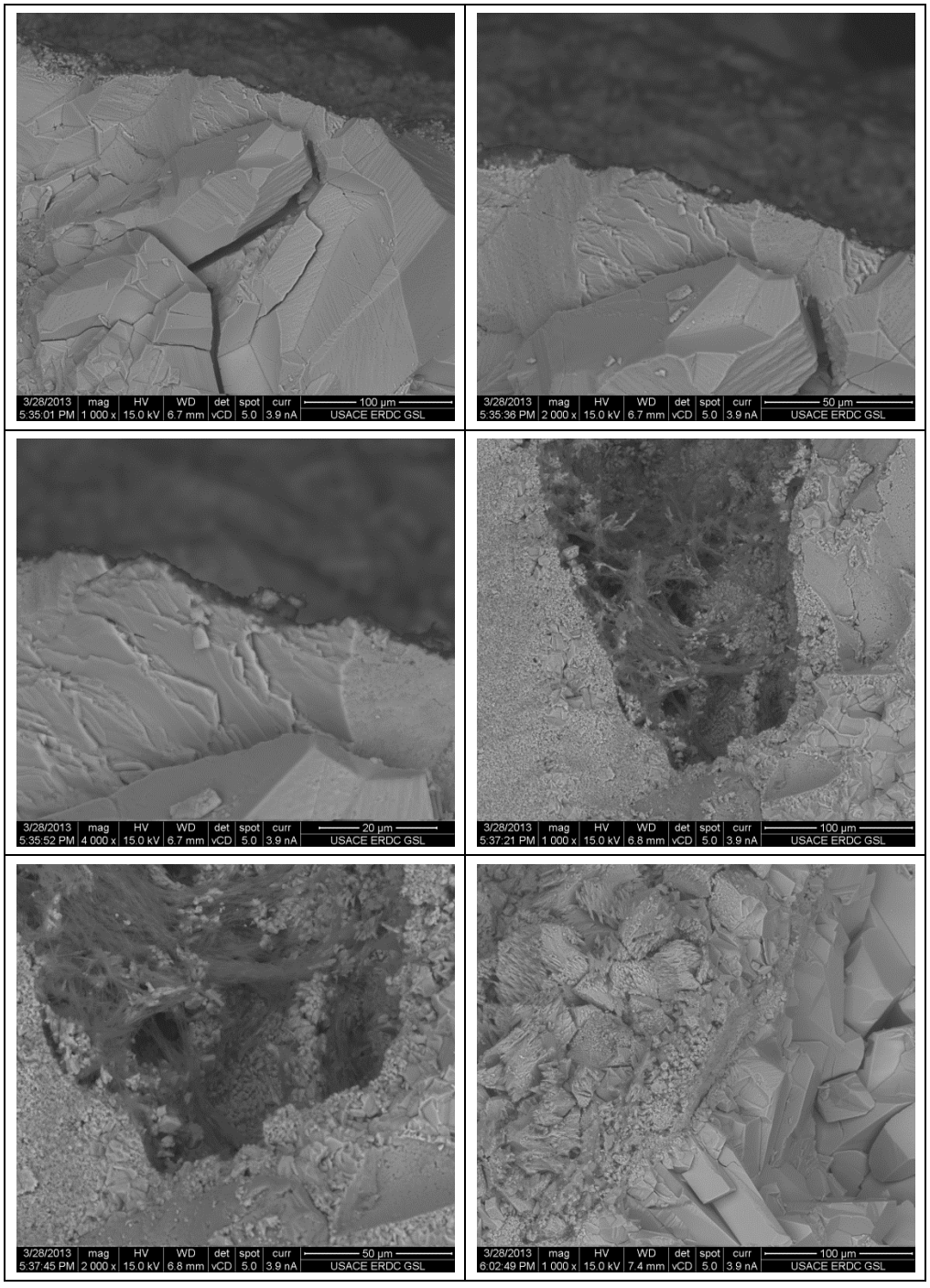

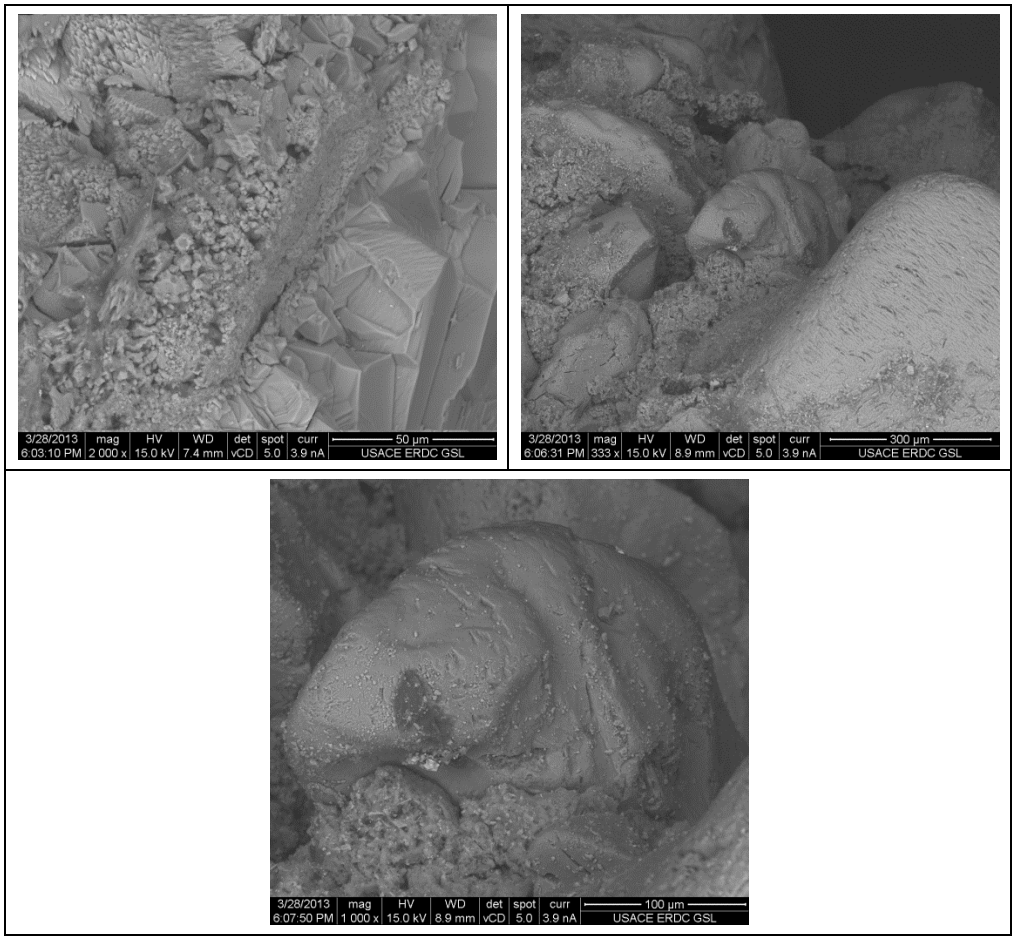
3/28/2013 | mag | HV | WD | det | spot | curr | 50 µm
6:03:10 PM | 2 000 x | 15.0 kV | 7.4 mm | vCD | 5.0 | 3.9 nA | USACE ERDC GSL
3/28/2013 | mag | HV | WD | det | spot | curr | 300 µm
6:06:31 PM | 333 x | 15.0 kV | 8.9 mm | vCD | 5.0 | 3.9 nA | USACE ERDC GSL
3/28/2013 | mag | HV | WD | det | spot | curr | 100 µm
6:07:50 PM | 1 000 x | 15.0 kV | 8.9 mm | vCD | 5.0 | 3.9 nA | USACE ERDC GSL

Figure B3. Supplemental SEM micrographs of exposed deteriorated concrete surface.

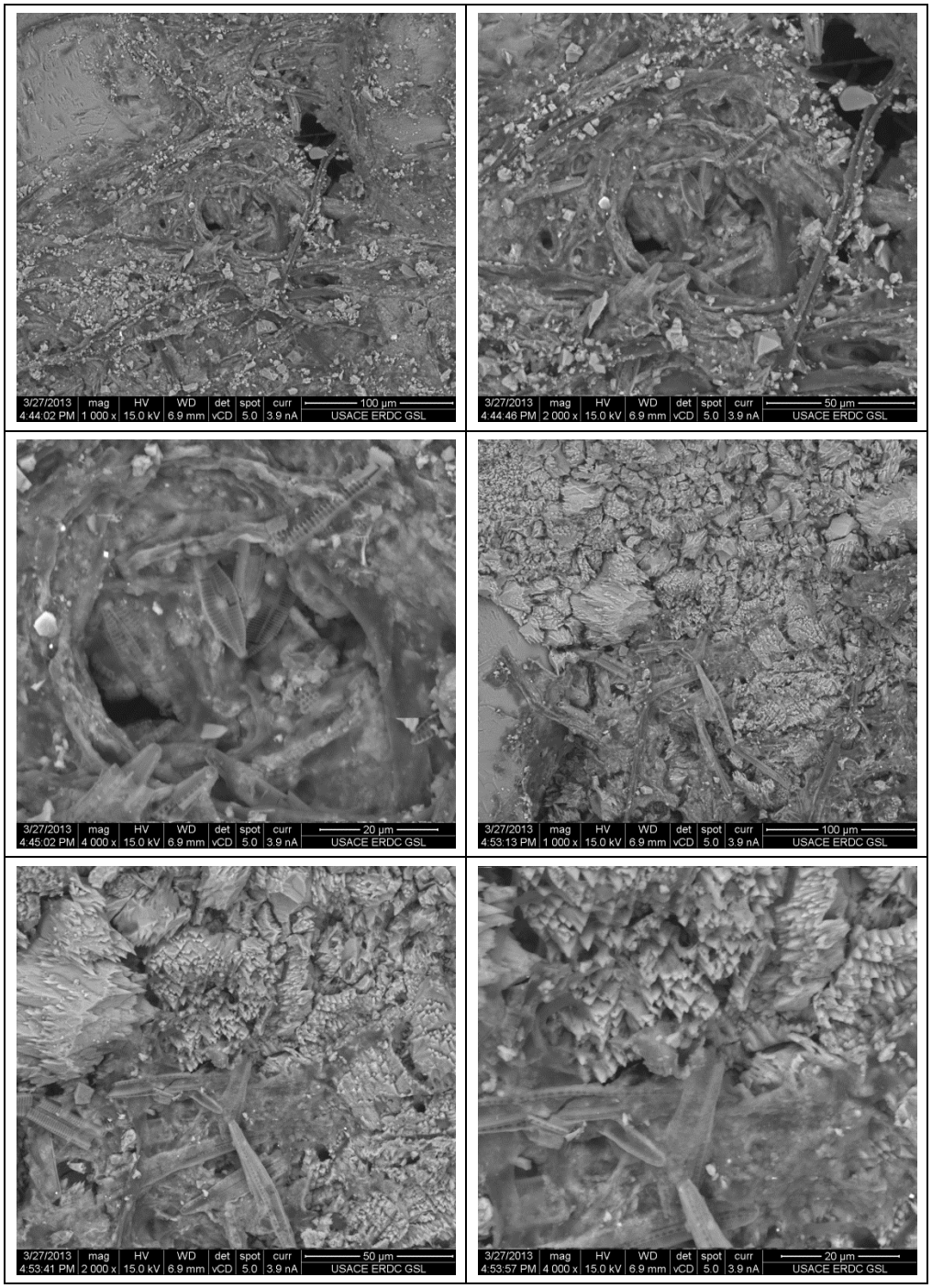

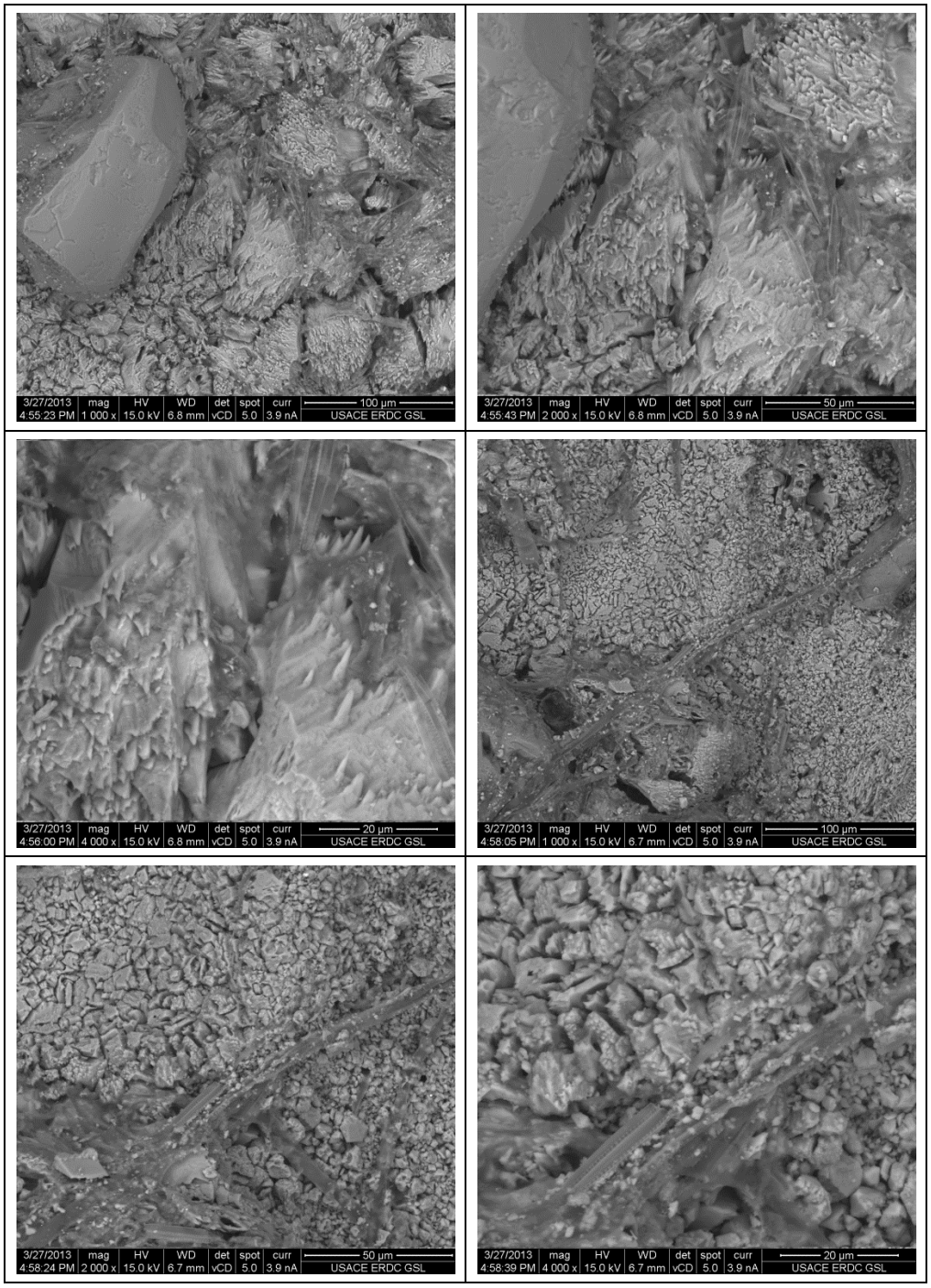
3/27/2013 mag HV WD det spot curr 100 µm
4:55:23 PM 1 000 x 15.0 kV 6.8 mm vCD 5.0 3.9 nA USACE ERDC GSL
3/27/2013 mag HV WD det spot curr 50 µm
4:55:43 PM 2 000 x 15.0 kV 6.8 mm vCD 5.0 3.9 nA USACE ERDC GSL
3/27/2013 mag HV WD det spot curr 20 µm
4:56:00 PM 4 000 x 15.0 kV 6.8 mm vCD 5.0 3.9 nA USACE ERDC GSL
3/27/2013 mag HV WD det spot curr 100 µm
4:58:05 PM 1 000 x 15.0 kV 6.7 mm vCD 5.0 3.9 nA USACE ERDC GSL
3/27/2013 mag HV WD det spot curr 50 µm
4:58:24 PM 2 000 x 15.0 kV 6.7 mm vCD 5.0 3.9 nA USACE ERDC GSL
3/27/2013 mag HV WD det spot curr 20 µm
4:58:39 PM 4 000 x 15.0 kV 6.7 mm vCD 5.0 3.9 nA USACE ERDC GSL

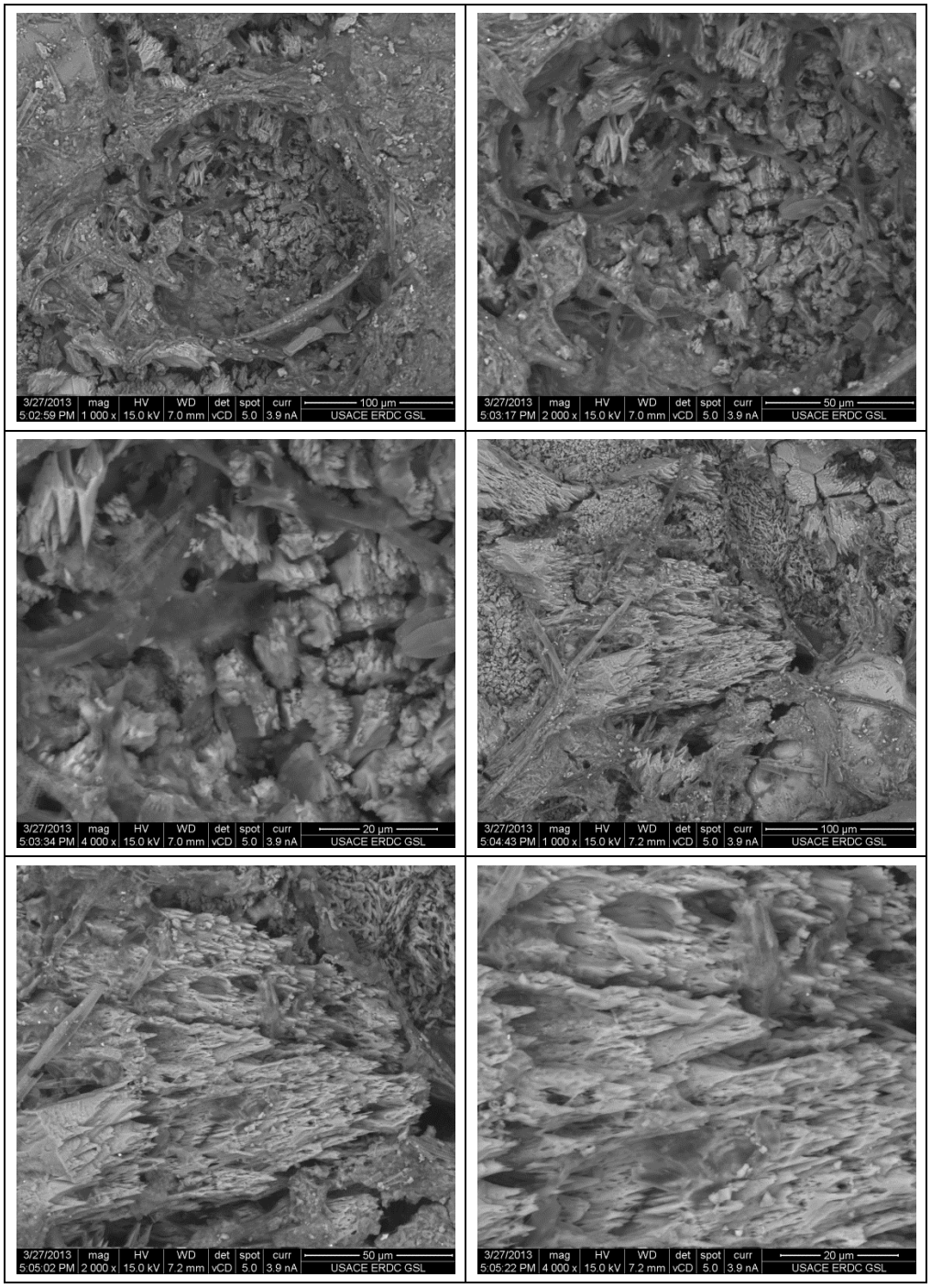
3/27/2013 5:02:59 PM mag 1 000 x HV 15.0 kV WD 7.0 mm det vCD spot 5.0 curr 3.9 nA 100 µm USACE ERDC GSL
3/27/2013 5:03:17 PM mag 2 000 x HV 15.0 kV WD 7.0 mm det vCD spot 5.0 curr 3.9 nA 50 µm USACE ERDC GSL
3/27/2013 5:03:34 PM mag 4 000 x HV 15.0 kV WD 7.0 mm det vCD spot 5.0 curr 3.9 nA 20 µm USACE ERDC GSL
3/27/2013 5:04:43 PM mag 1 000 x HV 15.0 kV WD 7.2 mm det vCD spot 5.0 curr 3.9 nA 100 µm USACE ERDC GSL
3/27/2013 5:05:02 PM mag 2 000 x HV 15.0 kV WD 7.2 mm det vCD spot 5.0 curr 3.9 nA 50 µm USACE ERDC GSL
3/27/2013 5:05:22 PM mag 4 000 x HV 15.0 kV WD 7.2 mm det vCD spot 5.0 curr 3.9 nA 20 µm USACE ERDC GSL

REPORT DOCUMENTATION PAGE

Form Approved
OMB No. 0704-0188

Public reporting burden for this collection of information is estimated to average 1 hour per response, including the time for reviewing instructions, searching existing data sources, gathering and maintaining the data needed, and completing and reviewing this collection of information. Send comments regarding this burden estimate or any other aspect of this collection of information, including suggestions for reducing this burden to Department of Defense, Washington Headquarters Services, Directorate for Information Operations and Reports (0704-0188), 1215 Jefferson Davis Highway, Suite 1204, Arlington, VA 22202-4302. Respondents should be aware that notwithstanding any other provision of law, no person shall be subject to any penalty for failing to comply with a collection of information if it does not display a currently valid OMB control number. **PLEASE DO NOT RETURN YOUR FORM TO THE ABOVE ADDRESS.**

1. REPORT DATE *(DD-MM-YYYY)*	**2. REPORT TYPE**	**3. DATES COVERED** *(From - To)*
February 2014	Final report	

4. TITLE AND SUBTITLE

An Investigation of Concrete Deterioration at South Florida Water Management District Structure S65E

5a. CONTRACT NUMBER

5b. GRANT NUMBER

5c. PROGRAM ELEMENT NUMBER

6. AUTHOR(S)

Robert D. Moser, E. Rae Gore, Charles A. Weiss Jr., and Brian H. Green

5d. PROJECT NUMBER

5e. TASK NUMBER

5f. WORK UNIT NUMBER

7. PERFORMING ORGANIZATION NAME(S) AND ADDRESS(ES)

US Army Engineer Research and Development Center
Geotechnical and Structures Laboratory
3909 Halls Ferry Road
Vicksburg, MS 39180-6199

8. PERFORMING ORGANIZATION REPORT NUMBER

ERDC/GSL TR-14-4

9. SPONSORING / MONITORING AGENCY NAME(S) AND ADDRESS(ES)

US Army Engineer District, Jacksonville
701 San Marco Blvd, Ste 4W, Jacksonville, FL

10. SPONSOR/MONITOR'S ACRONYM(S)

11. SPONSOR/MONITOR'S REPORT NUMBER(S)

12. DISTRIBUTION / AVAILABILITY STATEMENT

Approved for public release; distribution is unlimited.

13. SUPPLEMENTARY NOTES

14. ABSTRACT

This report documents the findings of a concrete deterioration study of South Florida Water Management District Structure S65E. The study examined water quality at the S65E site and concrete cores from deteriorated, repaired, and non-deteriorated areas of the structure. In addition, a geochemical water-rock reaction simulation was performed to investigate the potential for dissolution of the concrete based on local water quality. The predominant form of deterioration observed was severe loss of both paste and coarse aggregates from the surface of the concrete with larger losses in high-flow areas of dam piers than in the lock chamber. Concrete from deteriorated areas exhibited significant loss of Pleistocene limestone coarse aggregates and paste, while the siliceous, fine aggregates were unaffected. Concrete distress may be caused by dissolution of soluble phases and biodeterioration, which can result in localized acidification at the surface and direct or chemical consumption of mineral phases present in concrete. The use of siliceous aggregates, along with efforts to minimize porosity / permeability, and improved acid resistance would likely improve the durability of the repair material, as well as better protect the underlying concrete from subsequent deterioration.

15. SUBJECT TERMS

Concrete
Durability
Deterioration
Water quality
Aggregate
Lock
Dam

16. SECURITY CLASSIFICATION OF:			**17. LIMITATION OF ABSTRACT**	**18. NUMBER OF PAGES**	**19a. NAME OF RESPONSIBLE PERSON**
a. REPORT	**b. ABSTRACT**	**c. THIS PAGE**			**19b. TELEPHONE NUMBER** *(include area code)*
UNCLASSIFIED	UNCLASSIFIED	UNCLASSIFIED		53	